

**HIGH TEMPERATURE MECHANICAL AND MATERIAL PROPERTIES OF
BURNT MASONRY BRICKS**



by

Muhammad Farrukh Bashir

(2011 – NUST – MS PhD – Str – 10)

Master of Science

in

Structural Engineering

NUST Institute of Civil Engineering (NICE)

School of Civil and Environmental Engineering (SCEE)

National University of Sciences and Technology (NUST)

Islamabad, Pakistan

(2015)

This is to certify that the

thesis titled

**HIGH TEMPERATURE MECHANICAL AND MATERIAL PROPERTIES OF
BURNT MASONRY BRICKS**

submitted by

Muhammad Farrukh Bashir

(2011 – NUST – MS PhD – Str – 10)

has been accepted towards the partial fulfillment
of the requirements for the degree

of

MASTER OF SCIENCE

in

STRUCTURAL ENGINEERING

Dr. Wasim Khaliq
Associate Professor
NUST Institute of Civil Engineering (NICE)
School of Civil and Environmental Engineering (SCEE)
National University of Sciences and Technology (NUST), Islamabad,
Pakistan

ABSTRACT

Fire hazard is one of the most severe environmental conditions to which buildings and dwellings may be subjected, therefore, the provision of appropriate fire safety measures is an important aspect in-built infrastructure. In recent years there have been an increased research in fire performance of both normal strength concrete (NSC) and high strength concrete (HSC) for structural members in buildings and built infrastructure. On the other hand, burnt bricks are either used partially or as a major portion in structures around the world, however, the studies on fire performance of burnt bricks are scarce. There are also no studies available on comparative fire performance of burnt bricks to that of NSC or HSC. A test program was designed to undertake high temperature tests on burnt bricks commonly used in buildings and domestic construction. Mechanical properties namely compressive strength, tensile strength, elastic modulus, and compressive toughness were investigated at elevated temperatures (hot state) from 20°C to 800°C. These tests were done according to ASTM and RILEM test procedures. Results from high temperature experiments show that burnt bricks lose compressive strength in a manner similar to that of NSC and HSC. The measured tensile strength of burnt bricks is quite low as compared to compressive strength, with a very little gain around 200°C. High temperature properties also exhibit high reduction in stress-strain response of these bricks with increase in temperature. It was also observed that the failure response of bricks under stress changes from very stiff to soft with increasing temperatures and no spalling phenomenon was observed in burnt masonry bricks. Scanning electron microscope and X-ray fluorescence analysis of burnt bricks were also carried out to differentiate the microstructural and mineral changes that take place at elevated temperatures. To provide high temperature material properties of burnt bricks for analytical studies, data generated from mechanical property tests was utilized to develop simplified mathematical expressions as a function of temperature.

DEDICATION

To Mr. & Mrs. Bashir Ahmad

ACKNOWLEDGMENTS

I am grateful to Almighty Allah whose blessings gave me the strength to complete this research.

I bestow my sincere thanks to my advisor and mentor Dr. Wasim Khaliq, Associate Professor, NUST Institute of Civil Engineering for his advice, untiring guidance, incredible patience and supervision. He inspired me through his punctuality, professionalism, diligence, and sincerity.

I am grateful to him for his encouragement and motivation. He always urged me to achieve the best. All the credit goes to him for making me hard worker, focus and ambitious.

I extend my gratitude and special thanks to research committee members Dr. Syed Ali Rizwan, Dr. Shaukat Ali Khan and Dr. Khaliq-ur-Rashid Kiyani for their guidance during research. I also acknowledge the support of structures, SEM, XRF, XRD and TTL lab staff and students Saqib Hussain, Riasat Malik, Mohammad Ismail, Adnan Siddique and Aftab Ahmad for my extensive experimental work and especially Dr. Amir Habib SCME (NUST) for his advice. Finally, I am grateful to my colleagues Hammad Anis Khan and Syed Abid Hussain Zaidi for their sincere help and support during my research work.

TABLE OF CONTENTS

List of Tables	viii
List of Figures	ix
Chapter 1	1
1 Introduction.....	1
1.1 General	1
1.2 Fire Response of Burnt Masonry Bricks (BB)	2
1.3 Comparison of Mechanical Properties of Burnt Masonry Bricks With Normal Strength Concrete (NSC) and High Strength Concrete (HSC) ...	6
1.4 Objectives	7
1.5 Research Tasks	7
1.6 Thesis Outline	8
Chapter 2	9
2 State-Of-The-Art Literature Review	9
2.1 General	9
2.2 Masonry under Fire	12
2.3 Mechanical Properties	13
2.3.1 Compressive Strength	13
2.3.2 Tensile Strength	14
2.3.3 Stress Strain Curves	15
2.3.4 Elastic Modulus	16
2.4 X-Ray Fluorescence (XRF)	16
2.4.1 X-Ray Fluorescence (XRF) for Mineral Characterization	16
2.5 X-ray Powder Diffraction (XRD)	17
2.6 Scanning Electron Micrographic Images (SEM)	18
Chapter 3	28
3 Test Program	28
3.1 General	28
3.2 Plan of Mechanical Property Experiments	28
3.3 Mechanical Properties Tests	29
3.3.1 Test Specimen	29
3.4 Test Apparatus	30
3.4.1 Splitting Tensile Strength	30
3.4.2 Compressive Strength	30
3.4.3 X-Ray Fluorescence (XRF)	31
3.4.4 X-ray Powder Diffraction (XRD) Analysis	31
3.4.5 Stress Strain Response	32
3.4.6 Electric Furnace	32
3.4.7 Fiberfrax Thermal Insulating Blanket	32

Chapter 4	40
4 Results and Discussion	40
4.1 General	40
4.2 Mechanical Properties	40
4.2.1 Compressive Strength	40
4.2.2 Tensile Strength	43
4.2.3 Stress Strain Curves	45
4.2.4 Elastic Modulus	47
4.3 X-Ray Fluorescence (XRF) Analysis	49
4.4 X-ray Powder Diffraction (XRD) Analysis	51
4.5 Microscopic Study of Surface Texture	52
4.6 High Temperature Material Property Relationships for Burnt Masonry Bricks	53
Chapter 5	67
5 Conclusions and Recommendations	67
5.1 General	67
5.2 Conclusions	67
5.3 Recommendations	68
References	70

LIST OF TABLES

Table 4.1-	High Temperature Unstressed Material Property Relationship for Burnt Masonry Bricks	55
Table 4.2-	Compressive Strength, Tensile Strength, Elastic Modulus, and Compressive Toughness Reduction Factors (B_t) at Different Temperatures for Burnt Masonry Bricks	55
Table 4.3-	Minerals Name, Composition and Reference Code Present in BB at 20°C Temperature	56
Table 4.4-	Minerals Name, Composition and Reference Code Present in BB at 800°C Temperature	57

LIST OF FIGURES

Fig 2.1-	Relative Compressive Strength of Burnt Masonry Bricks as a Function of Temperature	19
Fig 2.2 -	Relative Compressive Strength of Burnt Masonry Bricks Compared To NSC as a Function of Temperature	19
Fig 2.3 -	Relative Compressive Strength of Burnt Masonry Bricks Compared To HSC as a Function of Temperature	20
Fig 2.4 -	Comparison of Variation in Relative Tensile Strength of Burnt Masonry Bricks as a Function of Temperature	20
Fig 2.5 -	Variation in Relative Tensile Strength of NSC and Burnt Masonry Bricks as a Function of Temperature.....	21
Fig 2.6 -	Variation in Relative Tensile Strength of HSC and Burnt Masonry Bricks as a Function of Temperature	21
Fig 2.7 -	Effect of Temperature On Stress Strain Diagram of Concrete (Abrams 1971)	22
Fig 2.8 -	Stress Strain Diagrams of Bricks at Different Temperatures (Mbumbia and De Wilmars).....	22
Fig 2.9 -	Effect of Temperature On Stress Strain Diagram of Bricks (Ayala 2011) ..	23
Fig 2.10 -	Effect of Temperature On Stress Strain Diagram of Light Weight Concrete Blocks (Andreini and Sassu 2011)	23
Fig 2.11 -	Variation in Relative Elastic Modulus of Burnt Masonry Bricks as a Function of Temperature	24
Fig 2.12 -	Variation in Relative Elastic Modulus of Burnt Masonry Bricks as Compared To NSC at Elevated Temperatures	24
Fig 2.13 -	Variation in Relative Elastic Modulus of Burnt Masonry Bricks as Compared To HSC at Elevated Temperatures	25
Fig 2.14 -	SEM Micrographs versus Sintering Temp. a: Raw; B: 460 °C; C: 560°C; D: 1000 °C; and E: 1100 °C. M: Mullite; K: Kaolinite; and Q: Quartz	26
Fig 2.15 -	SEM Micrographs of Adobe Clayey Bricks Samples. (a) Lime Free Sample, (B) 4 Wt.% Lime, (C) 6 Wt.% Lime, (D and E) 10 Wt.% Lime and (F) 12 Wt.% Lime	27
Fig 3.1 -	Specimen for ASTM C 1314	33
Fig 3.2 -	Specimen for ASTM C 1006	33

Fig 3.3 - Specimen Wrapped in Polythene Bag for ASTM C 1314	34
Fig 3.4 - Specimen Wrapped in Polythene Bag for ASTM C 1314	34
Fig 3.5 - ASTM C 1006 Splitting Tensile Strength Apparatus	35
Fig 3.6 - Multifunctional Control Console MCC 82	35
Fig 3.7 - JEOL JSX-3202-M XRF Element Analyzer	36
Fig 3.8 - LVDT for Measuring Strain	36
Fig 3.9 - Data Logger	37
Fig 3.10 - Digimax	37
Fig 3.11 - Load Cell	38
Fig 3.12 - Electric Furnace with Temperature Range up to 800°C	38
Fig 3.13 - Fiberfrax Thermal Insulating Blanket	39
Fig 4.1 - Variation in Relative Compressive Strength of Burnt Masonry Bricks (Test Data) as a Function of Temperature	58
Fig 4.2 - Comparison of Variation in Relative Compressive Strength of Burnt Masonry Bricks as a Function of Temperature	58
Fig 4.3 - Relative Compressive Strength of HSC, NSC and Burnt Masonry Bricks as a Function of Temperature	59
Fig 4.4 - Relative Tensile Strength of Burnt Masonry Bricks as a Function of Temperature	59
Fig 4.5 - Comparison of Variation in Relative Tensile Strength of Burnt Masonry Bricks as a Function of Temperature	60
Fig 4.6 - Variation in Relative Tensile Strength of HSC, NSC and Burnt Masonry Bricks (BB) as a Function of Temperature	60
Fig 4.7 - High Temperature Stress Strain Curves of Burnt Masonry Bricks	61
Fig 4.8 - High Temperature Stress Strain Curves of Burnt Masonry Bricks	61
Fig 4.9 - Relative Elastic Modulus of Burnt Masonry Bricks as a Function of Temperature.....	62
Fig 4.10 - Variation in Relative Elastic Modulus of Burnt Masonry Bricks as a Function of Temperature	62
Fig 4.11 - Variation in Relative Elastic Modulus of Burnt Masonry Bricks as Compared To NSC at Elevated Temperatures	63
Fig 4.12 - Variation in Relative Elastic Modulus of Burnt Masonry Bricks as Compared To HSC at Elevated Temperatures	63

Fig 4.13 - XRF of Burnt Masonry Bricks at Different Temperatures 64

Fig 4.14 - XRD diffraction analysis of BB at 20°C temperature 64

Fig 4.15 - XRD diffraction analysis of BB at 800°C temperature 65

Fig 4.16 - SEM Micrographs of Burnt Masonry Bricks (BB) at Different
Temperatures 66

INTRODUCTION

1.1 General

The progress of human development has often been reckoned in terms of the material used by society, e.g. the Stone Age in the prehistoric period which progress through bronze, iron, and successively more sophisticated materials and their combination in this modern age. Early people used material largely as they were produced by nature, but today we have come to rely increasingly on engineered materials. Engineering professionals are busy trying to improve the quality design procedures since long but as different materials are evolved so the construction management which emphasize on the economy of structure so from prehistoric times to now-a-days burnt bricks are the cheapest construction material available.

The fire performance of any material depends upon its thermal and mechanical properties. Masonry has been used to construct significant structures since the beginning of civilization (Drysdale and Hamid 2005) for its durability and aesthetic reasons. In addition, fire and heat resistance and versatility make masonry, to this day, an appealing building material. However, the structural use of masonry experienced a decline in the past 100 years due to the slow development and implementation of rational design standards. While new construction techniques supported by design guidelines were developing for structural steel and reinforced concrete, the design of masonry was still largely based on the “rules of thumb” principles (Hatzinikolas and Y. Korany 2005).

Technological development in civil engineering is a very slow process and introduction of new materials and production methods often takes decades. Pakistan, being an under developed country needs to concentrate on saving resources, which can be effectively done by introducing new technologies in major fields by adopting quality design procedures. Many engineering design codes involve selection and manipulation of materials and many of these designs give priority to strength only but little importance is given to the serviceability of structure and one of the most important phenomena regarding serviceability is resistance against fire. The main concern of design codes is to make sure that resulting structure support applied loads without fracture or excessive deformation under loads as given by ASCE-07 but this standard gives no criteria regarding fire resistance properties of constituent materials.

Masonry has been used since the time immemorial but now-a-days cost has been very important because material cost money and the designer must use only enough material to satisfy the strength and serviceability requirements. Apart from new construction materials BBs as a construction material has undergone a continuous evolutionary process. In modern construction burnt bricks BBs are the cheapest available materials and the most important fact regarding fire resistance that they are non-combustible. BBs have enormous fire resistance capability. In frame construction it is common practice to use BBs as infill and partition walls. It is envisaged that the fire resistance capacity of concrete and will exhibit different fire behavior and load carrying capacity to that of concrete.

1.2 Fire Response of Burnt Masonry Bricks (BB)

When BBs are used in construction, they must have to satisfy fire resistance requirements of building and fire safety codes and standards. The knowledge of high temperature thermal and mechanical properties is critical for evaluating the fire response of buildings made of burnt bricks BBs. The fire performance of structural members is dependent on thermal and

mechanical properties of its constituent materials. Strength and stiffness properties of BBs and concrete deteriorate with increasing temperature.

Recently, work has been carried out by various researchers to study the fire performance of brick masonry (Andreini and Sassu 2011; Ayala 2011; Johari et al. 2010; Mbumbia et al. 2000; Nadjai et al. 2003; Nguyen et al. 2009; Russo and Sciarretta 2013; Sandoval et al. 2011; Xiao et al. 2013). These studies mostly furnish excellent fire performance data for brick masonry, however the test results corresponds to post-fire (residual property) conditions. The residual properties data usually do not depict true performance of structures under fire conditions for which, the material properties data at elevated temperatures is required.

Masonry bricks are used in almost all types of building construction in many parts of the world being economical material, good acoustic and heat insulation properties, easy availability and require less involvement of skilled labor. Because of these advantages many types of bricks are introduced which can be either solid or hollow which are made from different materials like fired clay, concrete, calcium silicate or natural stone. These exhibit elastic-brittle properties with compressive strength in the range of 20 MPa to 100 MPa for fired clay unit, 10 MPa to 30 MPa for concrete and calcium silicate units and 3 MPa to 5 MPa for autoclaved aerated concrete units.

Masonry has been used since ages and it has proved itself a well-established material. It has been utilized many important and famous structures in the world which are made up of masonry like in prehistoric times such as, Stonehenge in southern England, the Great Sphinx of Egypt, and the pyramids of Giza, Parthenon of Greece and the Colosseum of Rome. While in Europe there is present St. Mark's cathedral in Venice, the palace of Alhambra in Spain, the Tower of London, the Dumo in Florence and the Vatican city of Rome. In Asia, the masonry structures which give proof that masonry is a durable building material are the Taj Mahal in India, Petra

city in Jordan, the Tomb of Humayun in Delhi, the Blue Mosque at Tabriz, the sanctuary of Cambodia the Angkor Wat and the Great Wall of China. These are few examples which confirm and established masonry as well seasoned, durable, reliable and long lasting material.

Like most developing countries, concrete frame structures are commonly built as main frame and BBs are used as infill and partition walls. Though the commercial use of burnt bricks BBs is being practiced. In construction industry, the fire response of BBs is not taken into account.

These properties have to be known for evaluation of fire response of structures. So the structural response of BBs evaluation of mechanical properties such as compressive strength, splitting tensile strength and elastic modulus is desired. Very little research is available in the field of masonry related building materials particularly in the case of burnt bricks. The constituent and shape of the masonry are altered as per need but to enhance its mechanical properties or to disabilities, there is little work.

Among the mechanical properties the compressive strength of brick masonry is most important. When we talk about the durability of brick masonry fire resistance is also an important factor. Thermal properties include thermal conductivity, specific heat, thermal diffusivity, and thermal expansion and deformation properties such as creep and mechanical properties such as compressive strength, splitting tensile strength, and elastic modulus significantly influence fire response of a structural system. But our main concern is evaluation of mechanical properties such as compressive strength, splitting tensile strength, and elastic modulus under fire conditions.

In recent years many incidents have taken place in Pakistan. In 2012 at Karachi garment factory, fire killed 298 workers (Mansoor 2012). At Lahore in 2012 the shoe making factory caught fire which damaged the building a lot. In 2013 at LDA plaza Lahore fire destroyed the

building and eight people were killed. There are few of the fire accidents which suggest the need for incorporation of fire safety design in building infrastructure of Pakistan.

Therefore considering fire resistance of buildings, the behavior of building materials at elevated temperatures is of supreme importance to engineers so that they can build structures. Among the construction materials concrete and BBs are widely used in construction. The fire behavior of conventional concrete has been excessively interesting and it is that concrete loses its strength at elevated temperatures (Khaliq Wasim and Kodur Venkatesh 2011). However, there is very little data on fire response of BBs.

Every building code contains minimum fire protection requirements based on a combination of knowledge of the physical properties and past experience of the behavior of various construction materials when exposed to fire and upon fire endurance ratings specified by the survival times of specific structural assemblies or components in standard laboratory fire tests. Usually only the ambient temperature regime to a maximum is controlled in these tests. Therefore such tests do not give much information about the effect of specific high temperatures on the properties of the construction material such as concrete, its constituent materials, or reinforcing steel except in a very general way but there is no information available regarding mechanical properties of burnt bricks at elevated temperature.

To improve the fire resistance in building design more needs to be known about the thermal and mechanical properties of its constituent materials at elevated temperatures. It is relatively easy to determine the residual properties by standard test methods and the results provide much of the information needed to determine what can be saved after a fire.

1.3 Comparison of Mechanical Properties of Burnt Masonry Bricks With Normal Strength Concrete (NSC) and High Strength Concrete (HSC)

The material behavior of BBs is necessary to be compared to NSC and HSC as BBs are in conjunction with concrete quite often. Stress-strain curves results for HSC at elevated temperatures shows the increase in strains for carbonate aggregates is larger than that for siliceous aggregates and the strain at peak loading increases with temperature (Cheng et al. 2004). Mechanical properties and microstructure of high strength concrete containing polypropylene fibers exposed to elevated temperatures resists spalling significantly but the mechanical properties are slightly altered (Noumowe 2005). The fire resistance of normal strength concrete (NSC) is higher than high strength concrete (HSC) and use of propylene fibers and carbonate aggregates improve the fire resistance (Kodur et al. 2003).

The compressive and flexural strength of NSC and HSC decreases with increasing temperature, and the decline in strength is more significant in HSC as compared to NSC (Husem 2006). The mechanical properties of self-consolidating concrete (SCC) and fiber reinforced SCC (FRSCC) in the temperature range of 20 to 800°C, shows that the presence of steel fibers enhances high temperature splitting tensile strength and elastic modulus of SCC. The high temperature mechanical properties of high strength fly ash concrete with and without fibers was investigated by (Khaliq and Kodur 2012) the mechanical properties were similar to that of high strength concrete (HSC).

1.4 Objectives

The objective of this research are;

- To study the mechanical properties of burnt bricks BBs at elevated temperature
- To compare such results, to the extent possible, with published information for conventional clay-based materials. The engineering properties include compressive strength, flexural tensile strength and modulus of elasticity of BBs at elevated temperature.
- To conduct X-ray fluorescence (XRF) to understand the chemical and mineralogical changes that take place in BBs at elevated temperature.
- Scanning electron microscopy (SEM) to visualize the microstructure
- Simple linear relations will be developed to predict the fire response behavior of structures made up of BBs.

1.5 Research Tasks

To accomplish research objectives following tasks are performed.

- Literature review
- Test set up which includes furnace, XRF, splitting tensile strength equipment
- Perform high temperature tests
- Find strength properties and make stress-strain graphs
- Evaluate and analyze experimental results
- Conclusions and recommendations

1.6 Thesis Outline

The research, undertaken to address the above objectives, is presented in seven chapters.

Chapter 1 provides some background about the masonry structures and its constituent materials. It discusses the mechanical and thermal properties of masonry. It provides some fire incidents history which emphasize the research objectives. It also mentioned that there is no standard procedures to determine the mechanical properties of burnt bricks at elevated temperature. Chapter 2 provides a state-of-the-art review of the mechanical properties of the masonry like compressive strength, tensile strength and modulus of elasticity. It also explore the stress-strain characteristics, mineralogical composition and scanning electron micrographs of masonry materials.

Chapter 3 deals with the test setup. It explains which type of equipment are used to measure the mechanical properties.

Chapter 4 presents an overview of the test procedure which describes the ways and methods to determine the mechanical properties.

Chapter 5 provides evaluation and analysis of tests and simple linear empirical high temperature relationships of BBs.

Chapter 6 provides detailed conclusion and remarks.

STATE-OF-THE-ART LITERATURE REVIEW

2.1 General

Not until 1950's, the introduction of the American Standards Association Building Code Requirements for Masonry (ACI Committee 318 2011) and the National Building Code of Canada (1965) (National Research Council of Canada 1965) began the revival of masonry. At present, there are various codes and standards worldwide governing the design of masonry structures, most of which are based on limit state design philosophy. In Canada, the governing standard is CSA S304.1-04 (2004) for design of masonry structures (Canadian Standard Association 2004) whereas in US, Standard Method for Determining Fire Resistance of Concrete and Masonry Construction Assemblies (ACI Committee 216 1997) is used.

As ASTM standards are available for evaluating mechanical properties but for thermal properties we seek help of RILEM test procedures.

(1) RILEM TC 129-MHT: test methods for mechanical properties of concrete at high temperatures Part 4: tensile strength for service and accident conditions (RILEM TC 129-MHT: Test methods for mechanical properties of concrete at high temperatures Part Part 4: tensile strength for service and accident conditions 2000). This document presents test parameters and test procedures for measuring the direct tensile strength of concrete cylinders in the longitudinal direction, either at high temperatures after first heating or after cooling.

(2) RILEM TC 129-MHT: test methods for mechanical properties of concrete at high temperatures Part 3: compressive strength for service and accident conditions (RILEM 1995).

This document presents test parameters and test procedures for measuring the compressive strength of concrete cylinders either at high temperatures after first heating or after cooling.

(3) RILEM TC 129-MHT: test methods for mechanical properties of concrete at high temperatures Part 5: modulus of elasticity for service and accident conditions (RILEM TC 129-MHT: Test methods for mechanical properties of concrete at high temperatures Part 5: modulus of elasticity for service and accident conditions 2004). This document presents test parameters and test procedures for measuring the modulus of elasticity of concrete cylinders at high temperatures after first heating or after cooling.

(4) RILEM TC 200-HTC: mechanical concrete properties at high temperatures Part 2: stress-strain relations (RILEM TC 200-HTC: Test methods for mechanical properties of concrete at high temperatures Part 2: stress-strain relations 2007). This document presents test parameters and test procedures for measuring the stress-strain relations of concrete either at high temperatures after first heating or after cooling. The temperature ranges from 20°C to 750°C or above, for all above parts of RILEM Recommendation.

The ACI committee and ASTM standard have following procedure for masonry bricks
Some of them are explained below.

ACI committee 216 “Standard Method for Determining Fire Resistance of Concrete and Masonry Construction Assemblies” (ACI Committee 216 1997) gives construction procedures against fire resistance but it did not mention about how to determine thermal and mechanical properties against fire resistance.

According to ASTM C 62-12 “Standard Specification for Building Brick (Solid Masonry Units Made From Clay or Shale)” different grades are introduced according to their

weather resistance capacities and they are classified with respect to their compressive strength at room temperature.

ASTM C 140-12 “Standard Test Methods for Sampling and Testing Concrete Masonry Units and Related Units” gives procedures for compressive procedures at room temperature only.

ASTM C 67-12 “Standard Test Methods for Sampling and Testing Brick and Structural Clay Tile” gives procedures not for compressive strength but for flexure strength also procedures at room temperature.

ASTM C 1006-12 “Standard Test Method for Splitting Tensile Strength of Masonry Units” This test method covers the determination of the splitting tensile strength of masonry units at room temperature.

ASTM C 1314-12 “Standard Test Method for Compressive Strength of Masonry Prisms” This test method covers procedures for masonry prism construction and testing, and procedures for determining the compressive strength of masonry.

ASTM E 119-12 “Standard Test Methods for Fire Tests of Building Construction and Materials” this standard uses two tests namely, fire endurance and hose stream test. Both tests utilize full structural member like beam, column and roof as a specimen and calculate time-temperature curve but not their compressive and flexure strength.

So, there are no reported studies carried out where effect of fire on individual BBs prisms can be studied. Moreover no guidance is provided how to determine the thermal and mechanical properties of BBs under fire conditions.

2.2 Masonry under Fire

According to the serviceability considerations, fire safety design is very important and fire resistance of building materials is intrinsic part of it because fire is a natural disaster and building structures are very prone to it. Masonry bricks have low thermal conductivity thus they produce high thermal gradient over the cross-section. It is non-combustible. It gives no smoke and toxic fumes under fire conditions. The main components of clay are silica and alumina which convert into kaolinite, metakalinite, quartz, illite and mullite. Their transformations depend upon the composition and temperature. Its excellent fire resistance properties are due to its constituent materials which undergo mineralogical transformations at elevated temperature. They decompose and absorb heat the water present in microscopic pores also lowers the temperature so its low thermal conductivity and high heat capacity provide good inherent fire resistance.

Although it is excellent fire resistance material but at elevated temperatures its strength decreases. The minerals melt and their matrix structure becomes altered. The matrix composed by minerals becomes less dense, empty spaces created in it, thus leading to strength loss. This reduction in strength is different for different masonry materials. A short description of the research work conducted by various researchers on the mechanical properties of masonry is represented below.

2.3 Mechanical Properties

The mechanical properties of BBs were obtained by using unstressed test method, the samples are directly transferred from the electric furnace to the strength test machine to evaluate their material properties without any loss of heat at specified target temperatures. This section presents the results of different material properties of BBs, NSC and HSC when exposed to elevated temperature using this test procedure.

2.3.1 Compressive Strength

Among mechanical properties, compressive strength of bricks has been investigated by many researchers (Andreini and Sassu 2011; Nadjai et al. 2003; Russo and Sciarretta 2012). (Andreini and Sassu 2011) developed an analytical model to determine the fire response of masonry panel when exposed to fire. In Fig. 2.1 the compressive strength of panel decreases as the temperature is increased. From room temperature to 400°C there is rapid decrease in compressive strength but in the range of 400-800°C the decreasing rate of compressive strength is low. The finite element model of masonry wall was formulated by Nadjai et al. (2003). The wall compressive strength characteristics of wall indicate that the compressive strength up to 400°C is decreasing slowly but after that it decreases rapidly up to 1200°C (Fig. 2.1). The comparison of mechanical properties of different types of bricks according to different codes like (Eurocode 6 2005), were presented by Russo and Sciarretta (2013). The masonry bricks were heated to 600°C as shown in Fig. 2.1. The rate of decrease of compressive strength is constant.

Enormous data is available on the compressive strength of NSC and HSC. The stress strain characteristics and development of micro cracks were studied by (Fu et al. 2004). He used compressive strength of composite concrete to generate the stress strain diagrams of concrete at elevated temperature. In Fig. 2.2 (Tang and Lo 2009) found the mechanical and fracture

properties of NSC blended with fly ash. In both cases (Fu et al. 2004; Tang and Lo 2009) the compressive strength decreases linearly with slow rate up to 400°C after that temperature it decreases rapidly (Fig. 2.2).

To reduce the dead load and reduce the structural element sizes much research has been carried out to enhance the compressive strength of concrete and a new era begun of concrete which generally named as high strength concrete HSC. To evaluate the fire resistance of HSC (Fu et al. 2005; Khaliq 2012) found the compressive strength of HSC at different elevated temperature. The compressive strength of HSC determined by (Fu et al. 2005) shows abrupt behavior up to 400°C there is not much decrease in the compressive strength but after that it decreases rapidly as shown in Fig. 2.3. From Fig. 2.3 the compressive strength of HSC found by (Khaliq 2012) shows smooth regular pattern of decrease of compressive strength.

2.3.2 Tensile Strength

Among mechanical properties the least evaluated property is the tensile strength but its importance cannot be ignored to determine the flexural strength of concrete. The flexure strength of masonry bricks concrete blocks found by (Xiao et al. 2013) to make the partition walls more sustainable indicate that the flexure strength remains constant up to 300°C after that it decreases rapidly as shown in Fig. 2.4. The analytical results of tensile strength of single leaf masonry walls determine by (Nadjai et al. 2003) shows that the tensile strength decreases almost with the same rate up to 800°C (Fig. 2.4).

The tensile strength of NSC and HSC is very important. This property gives us to assess the flexibility or ductility in such concrete types which is very crucial property while designing a structure in the earthquake prone areas and as the compressive strength of concrete increases it becomes more and more brittle. In Fig. 2.5 the tensile strength of NSC blended with fly ash was found by (Tang and Lo 2009) shows decrease of tensile strength as found by (Khaliq and

Kodur 2011) which shows smooth rate of decrease of tensile strength of NSC as shown in Fig. 2.5. Among HSC, the tensile strength found by (Behnood and Ghandehari 2009; Felicetti et al. 1996). The tensile strength of HSC decreases with the increase in the temperature (Fig. 2.6).

2.3.3 Stress Strain Curves

The stress strain diagrams are important parameters to know the behavior of material at different loading. The stress strain curves developed by (Abrams 1971) from compressive strength of concrete by varying different conditions like aggregate type and loading rates, indicate that the as the temperature is increased the stress strain curves becomes flat i.e., material gives more deformation at low load (Fig. 2.7).

The stress strain curves of masonry bricks found by (Mbumbia and de Wilmars 2002) shows different behavior the abrupt behavior can be explained on the basis of non-homogeneity of raw material of bricks. In Fig. 2.8 the curves are smaller but as the temperature is increased the curves shows more strain but overall trend shows that the post peak of curves always decrease as the temperature is increased.

The stress strain curves of masonry wallets found by (Ayala 2011) shows that the curves becomes flat and flatter as the temperature is increased which indicates that the strain is high at low stress level. Same trend is shown by (Andreini and Sassu 2011) as that of (Ayala 2011) except that curves do not show peak points. The curves becomes linear after reaching peak point indicating that at same stress level the strain is increased (Fig. 2.9-10).

2.3.4 Elastic Modulus

The elastic modulus of masonry bricks has been found by (Andreini and Sassu 2011; Russo and Sciarretta 2013) as shown in Fig. 2.11. Both the diagrams shows same trend of decrease of modulus. Up to 200°C the decrease in elastic modulus in rapid but as the temperature is increased the decreasing rate is low. The elastic modulus of NSC found by (Ayala 2011; Bažant 1996; Phan 2000; Schneider 1988) shows similar trend of decrease of elastic modulus i.e. as the temperature is increased the elastic modulus decreases (Fig. 2.12). In Fig. 2.13 the elastic modulus of HSC remains constant up to 200°C after that it decrease up to 800°C (Castillo and DurraniI 1990; Khaliq 2012; Phan 1996).

2.4 X-Ray Fluorescence (XRF)

The burnt masonry bricks are made from raw material which is composed of many minerals. The mechanical properties of BB are highly dependent on these minerals. To investigate the form, type and chemical and elemental formation an analytical technique called X-ray fluorescence (XRF) is used. This technique uses short wavelength to ionize the atoms of minerals. The ionization radiation of excited atoms was used to detect the atomic number of element. By using the same procedure minerals are spotted in the sample.

2.4.1 X-ray Fluorescence (XRF) for Mineral Characterization

Many researchers (Aramide 2012; Mbumbia and de Wilmars 2002; Mezencevova et al. 2012; Seynou et al. 2011) have investigated the mineralogical composition of masonry bricks or raw material of masonry bricks. The change in mechanical properties of masonry bricks by altering the firing temperature was investigated by (Aramide 2012). He uses XRF to know the different mineralogical and phase changes happened at elevated temperature. Some researchers like (Mbumbia and de Wilmars 2002) heated the bricks at low rate to determine the stress strain

characteristics of laterite bricks. XRF analysis was done to the mineralogical composition of laterite bricks and their effect on stress strain characteristics. To produce durable tiles with desired flexural strength and linear shrinkage (Seynou et al. 2011) mix different proportions of minerals in the mixture. The final product was analyzed with XRF to determine the mineralogical composition which impart desired properties to tiles. (Mezencevova et al. 2012) explore the suitability of river sediments by knowing the mineralogical composition of sediments through XRF.

2.5 X-ray Powder Diffraction (XRD)

XRD is the good technique to determine the mineral composition, International Center for Diffraction Data number (ICDD) and mineral name etc. The properties of bricks was analyzed by XRD after mixing the slag with masonry bricks. The firing temperature was reduced when the slag content was 10%. At 1100°C the sintering process begun. The main minerals were quartz, kaolin, magnesium aluminum silicate. The formation of quartz and kaolin decreased when the slag increased. Slag prevents the formation of new crystals (Shih et al. 2004). The chemical and mineralogical composition of castle building material was determine using XRD to help the administration in restoration activities. The weathering caused by salts was the main reason of deterioration of the castle. The identification of salts is done by XRD (Marrocchino et al. 2010). The changing in sintering process was investigated by XRD. The most abundant minerals present were quartz, illite and kaolinite. Firing transformations of clay along with properties of tiles confirms that the raw material should be amended with feldspar, sand or talc as fluxing agent to produce the required characteristics (Seynou et al. 2011).

2.6 Scanning Electron Microscopic Images (SEM)

Microscopically surface topography is used to understand the morphology of the sample when viewed under scanning electron microscope. Many researchers used this technique to know the morphological changes at the mineral level when the brick specimens were heated to elevated temperatures. (Seynou et al. 2011) determine the influence on mechanical properties of tiles when heated to elevated temperatures by knowing the mineralogical transformations observed under scanning electron microscope. Fig. 2.14 shows the firing transformations of minerals at different temperatures. Other researchers examine the morphology of bricks to know whether these are durable or not in conservation of historic buildings (Elert et al. 2003).

The influence of porosity of bricks on water absorption and drying behavior was observed by (Cultrone et al. 2004) under electron microscope to examine the different crystalline phases at different temperatures. The addition of varying amount of lime to bricks was done by (Millogo et al. 2008) to determine the suitability of bricks for construction. The influence of morphology on mechanical resistance of bricks was observed under scanning electron microscope. Fig. 2.15 shows SEM micrographs brick samples with varying amount of lime.

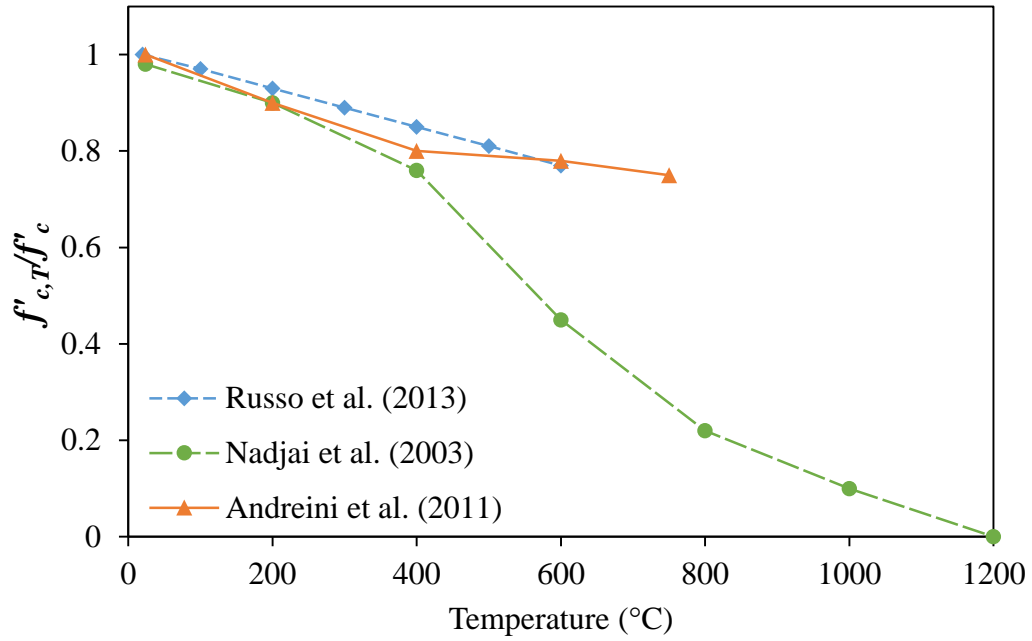


Fig 2.1: Relative compressive strength of burnt masonry bricks as a function of temperature

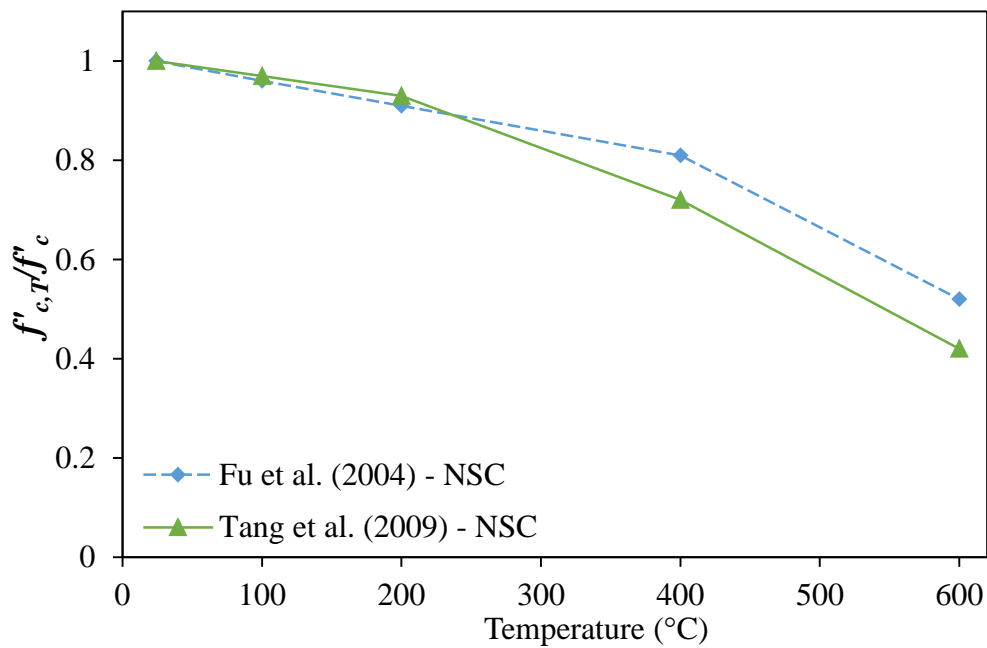


Fig 2.2: Relative compressive strength of burnt masonry bricks compared to NSC as a function of temperature

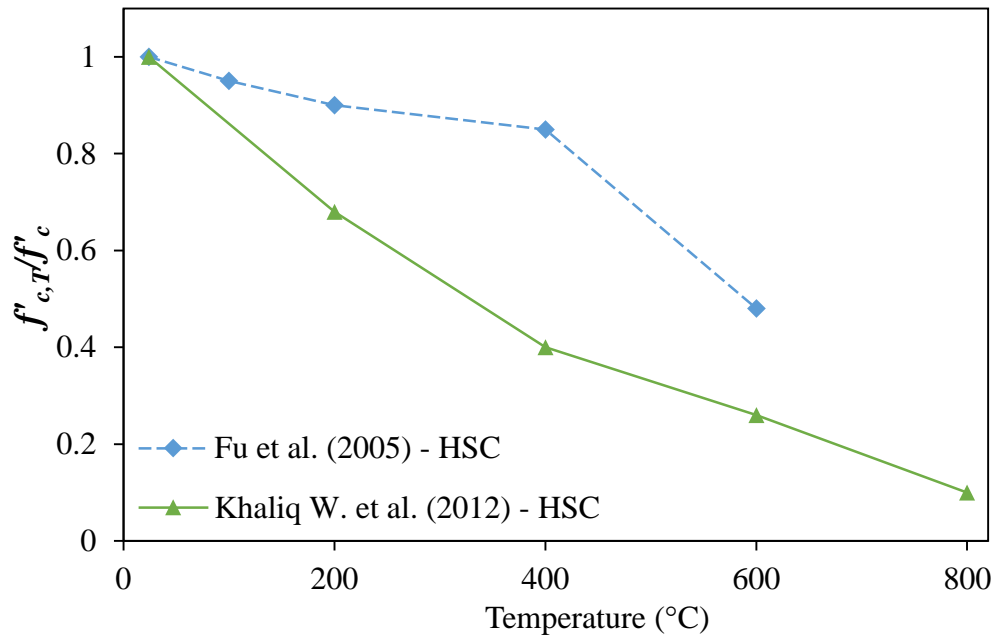


Fig 2.3: Relative compressive strength of burnt masonry bricks compared to HSC as a function of temperature

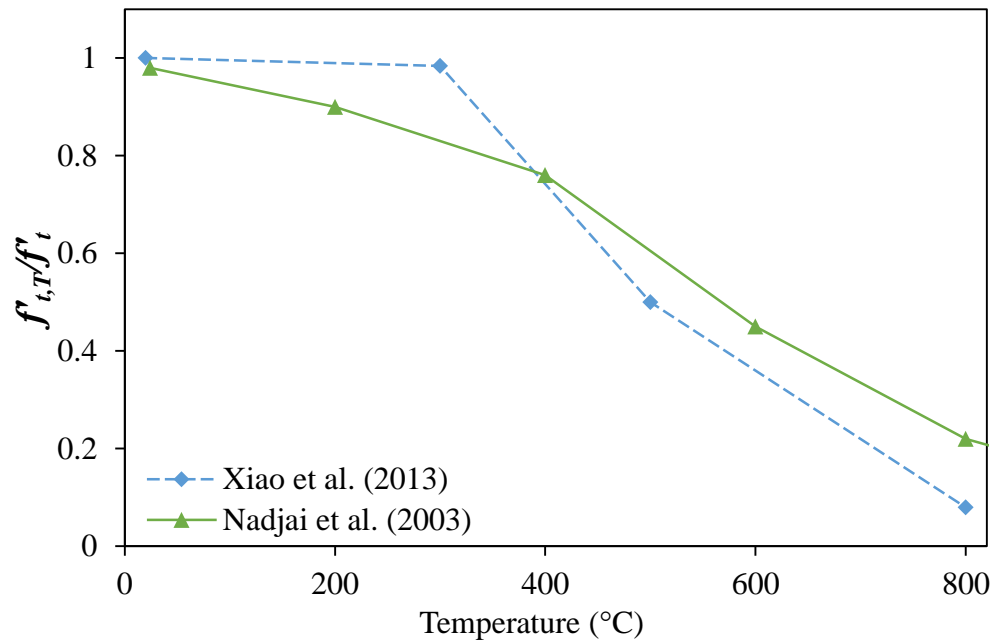


Fig 2.4: Comparison of variation in relative tensile strength of burnt masonry bricks as a function of temperature

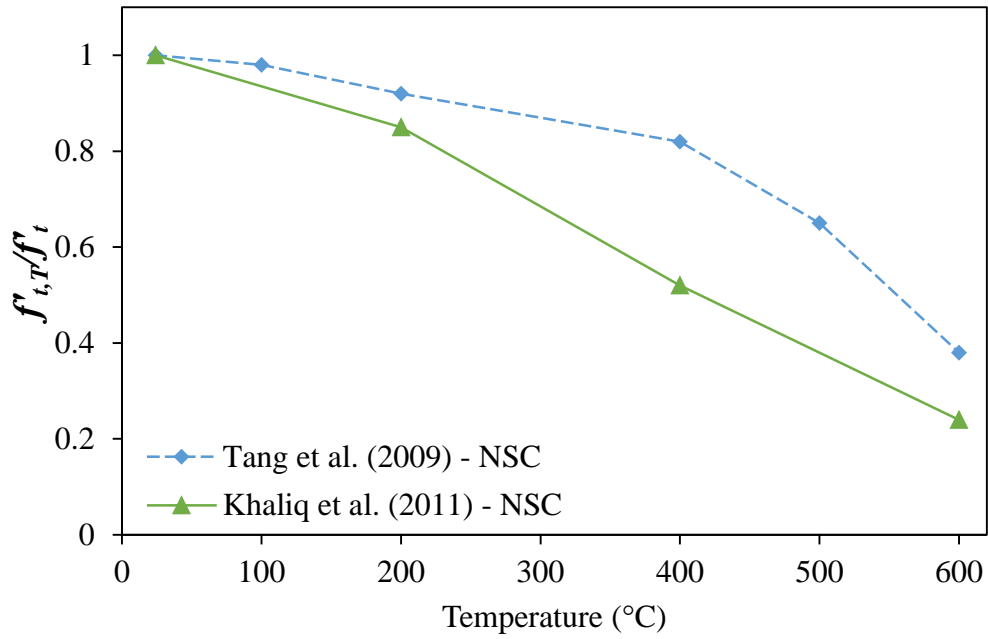


Fig 2.5: Variation in relative tensile strength of NSC and burnt masonry bricks as a function of temperature

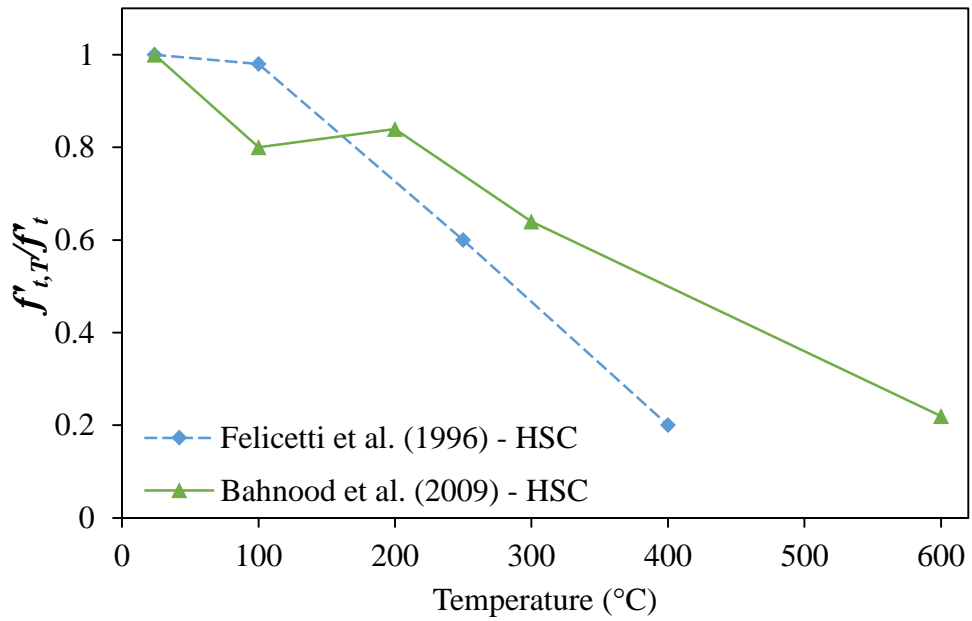


Fig 2.6: Variation in relative tensile strength of HSC and burnt masonry bricks as a function of temperature

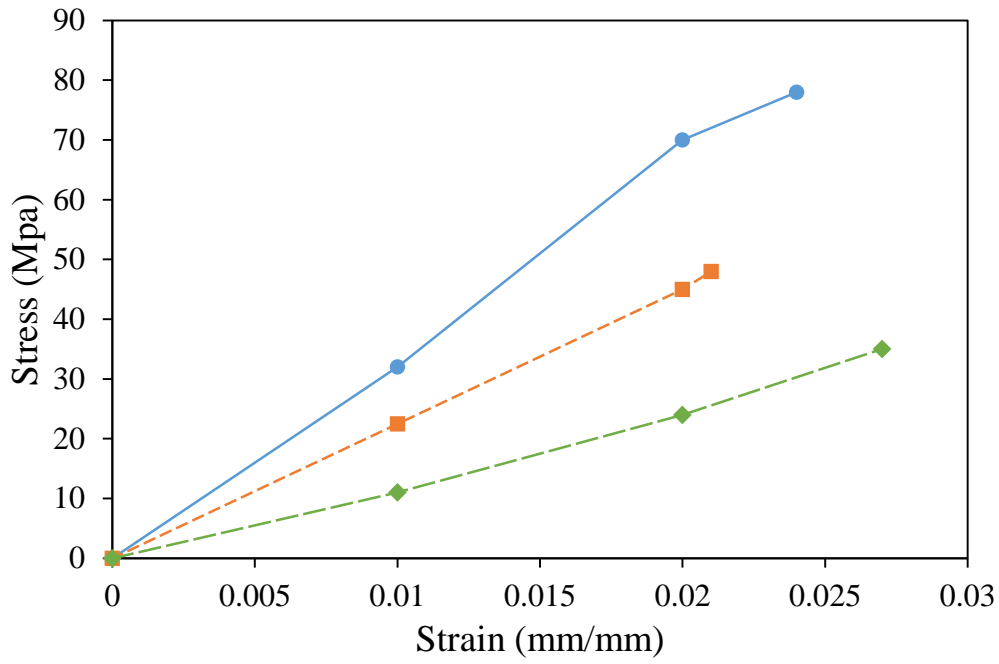


Fig 2.7: Effect of temperature on stress strain diagram of concrete (Abrams 1971)

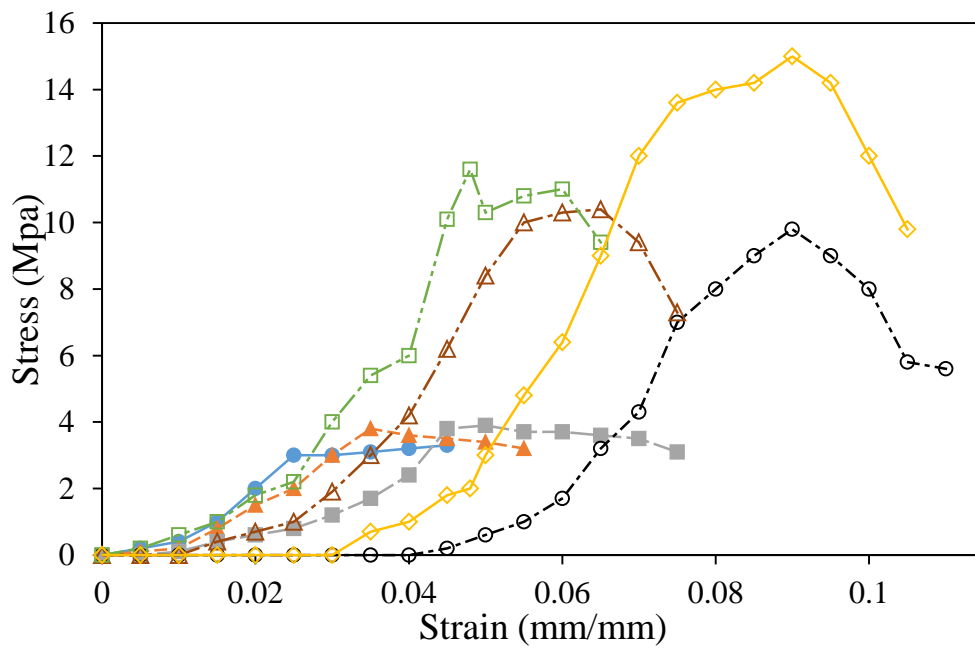


Fig 2.8: Stress strain diagrams of bricks at different temperatures (Mbumbia and de Wilmars 2002)

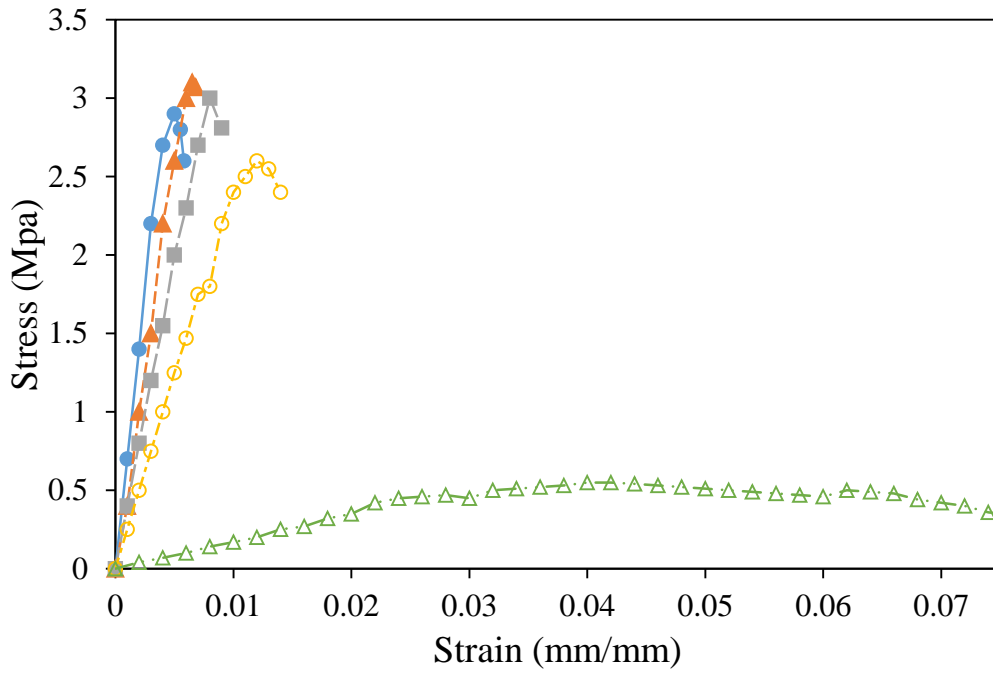


Fig 2.9: Effect of temperature on stress strain diagram of bricks (Ayala 2011)

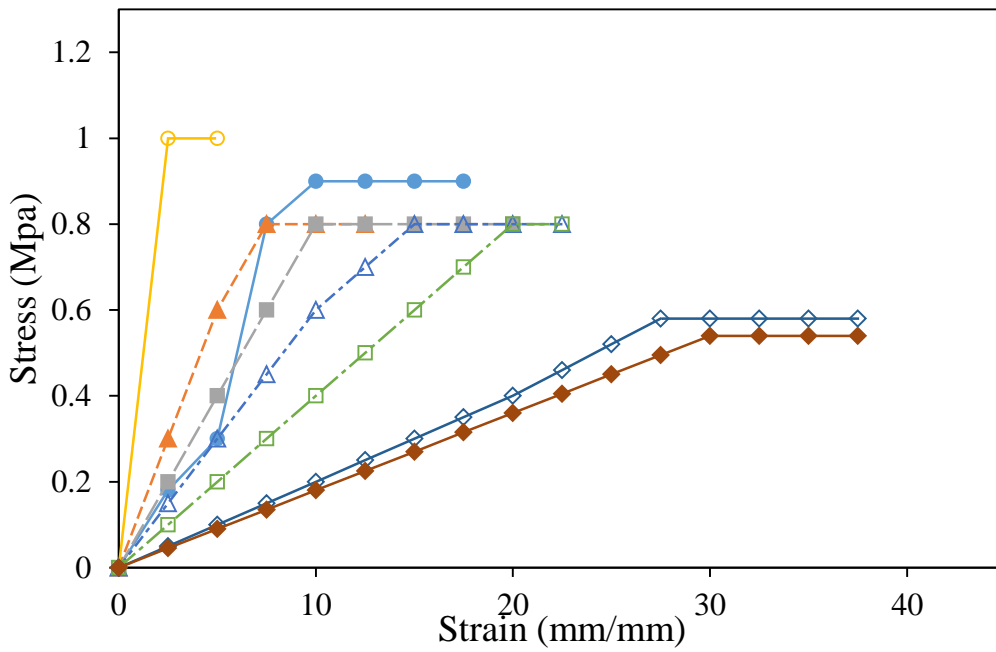


Fig 2.10: Effect of temperature on stress strain diagram of light weight concrete blocks (Andreini and Sassu 2011)

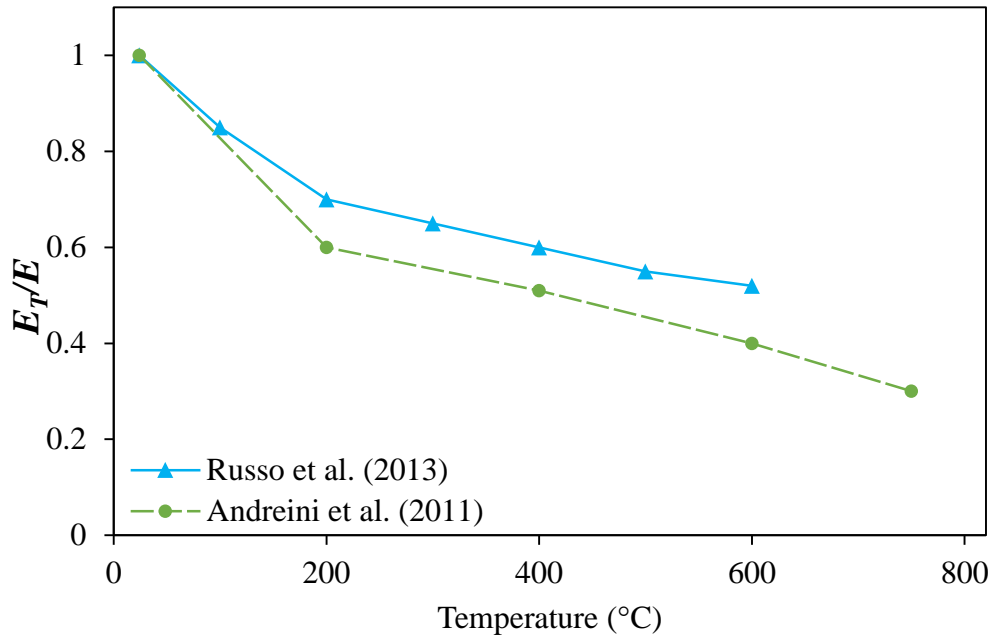


Fig 2.11: Variation in relative elastic modulus of burnt masonry bricks as a function of temperature

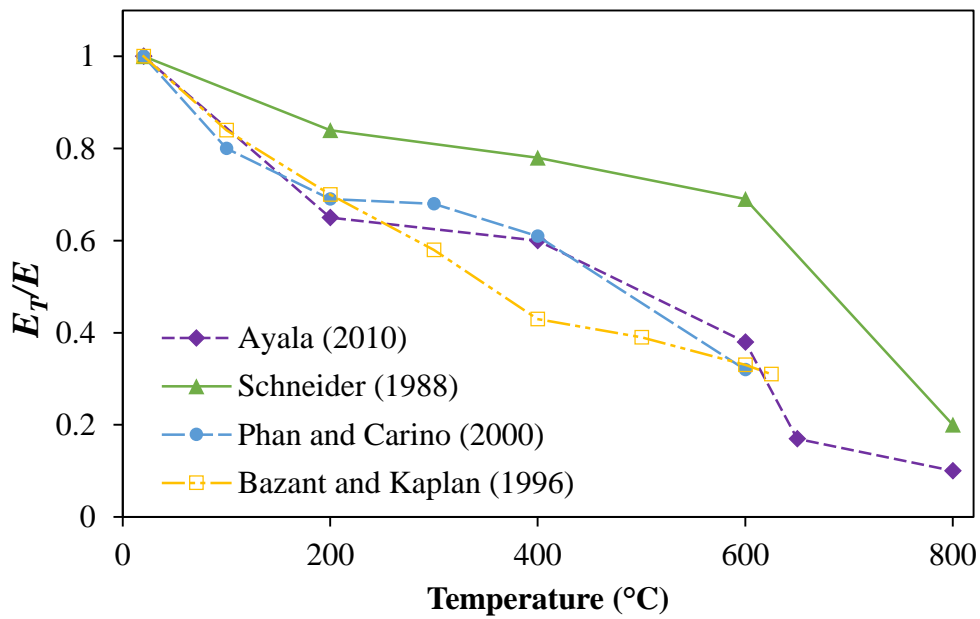


Fig 2.12: Variation in relative elastic modulus of burnt masonry bricks as compared to NSC at elevated temperatures

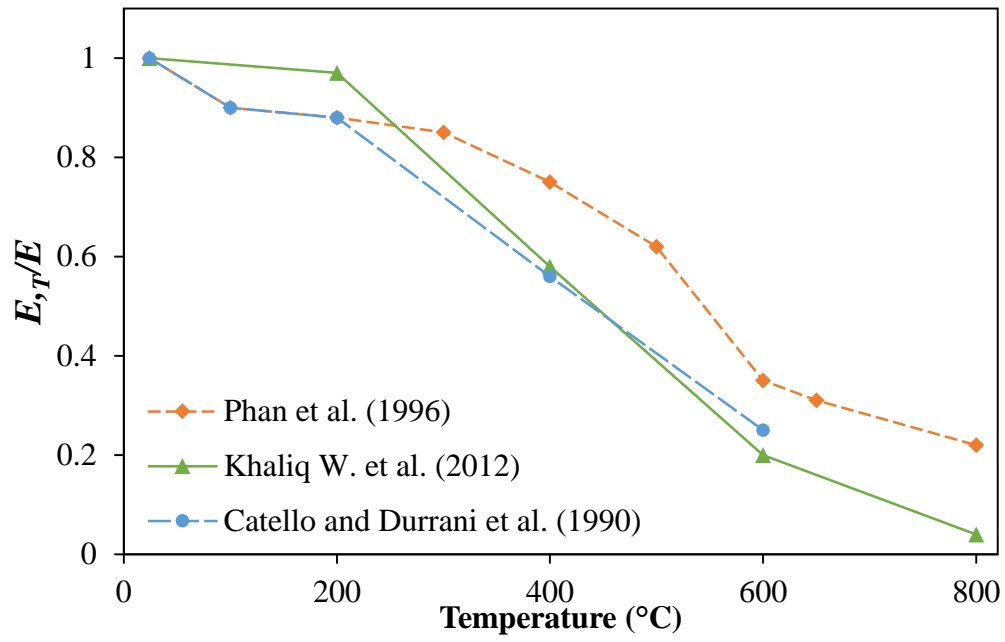


Fig 2.13: Variation in relative elastic modulus of burnt masonry bricks as compared to HSC at elevated temperatures

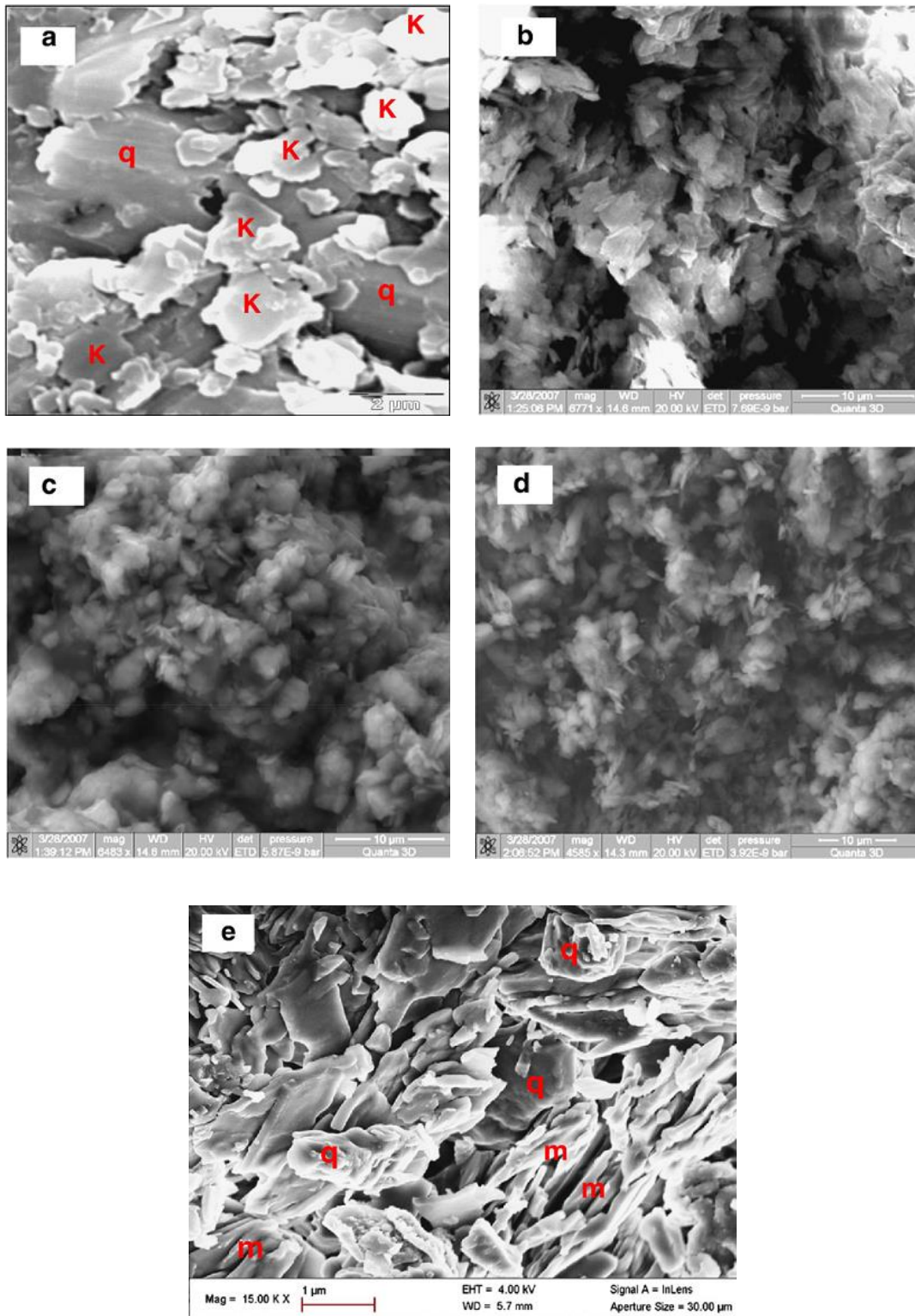


Fig 2.14: SEM micrographs versus sintering temperature. a: raw; b: 460 °C; c: 560 °C; d: 1000 °C; and e: 1100 °C; m: Mullite; k: Kaolinite; and q: Quartz (Seynou et al. 2011)

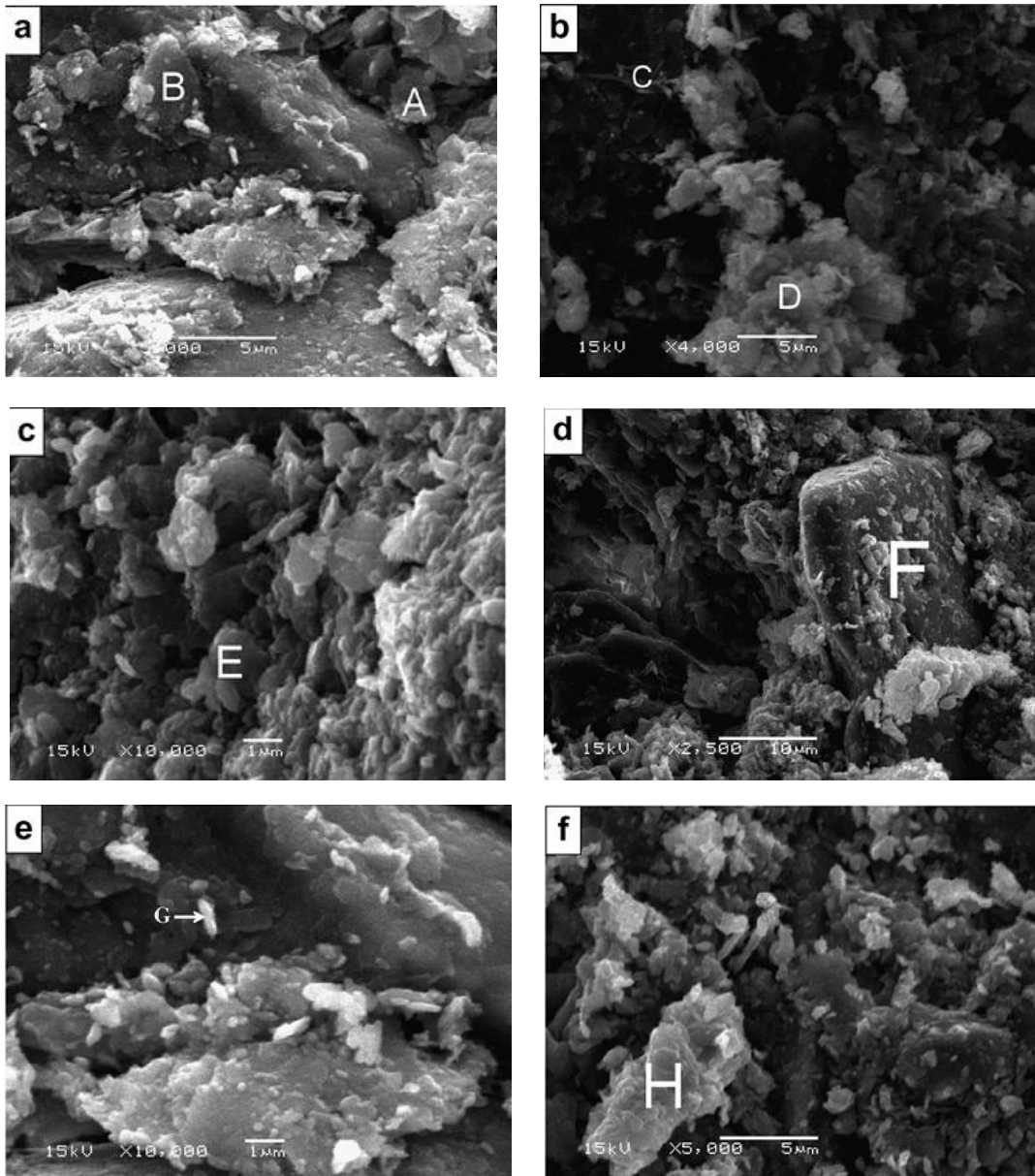


Fig 2.15: SEM micrographs of adobe clayey bricks samples. (a) Lime free sample, (b) 4 wt.% lime, (c) 6 wt.% lime, (d and e) 10 wt.% lime and (f) 12 wt.% lime (Millogo et al. 2008)

TEST PROGRAMME

3.1 General

The behavior of masonry under fire can only be explained with the help of mechanical properties at elevated temperature. The compressive strength, tensile strength and stress-strain curves are included in mechanical properties. The state-of-the-art review indicates that there is lack of data on the mechanical properties of burnt clay bricks at elevated temperatures. These properties are vital for evaluating the strength degradation of burnt clay bricks. The fire response of burnt clay bricks was evaluated by the high temperature property tests on compressive strength, tensile strength, modulus of elasticity and stress-strain were done. The experimental data generated from was applied to model the relations for various mechanical properties as a function of temperature. The temperature was in the range of 20°C to 800°C.

3.2 Plan of Mechanical Property Experiments

The test program was conceived to find out the high temperature mechanical property tests on burnt clay bricks of the same type. For the test, burnt clay bricks specimens were collected from the site. These specimens were tested at various temperature points in 20-800°C temperature range to evaluate mechanical properties.

There is no standardized test method is available for high temperature strength tests on burnt clay bricks in ASTM standards (ASTM C67-14 2014; ASTM C1006-07 2013; ASTM C1314-14 2014; ASTM E111-04 2010; ASTM E2309 2011) , RILEM (1995) (RILEM 1995) tests procedures were adopted to evaluate the mechanical properties of burnt clay bricks. To transfer the heated specimens to testing equipment special hand gripping tool was developed. To do

this a thermal jacket and insulated steel plate was used to transfer the specimens for compressive strength, splitting tensile strength tests and stress-strain tests.

3.3 Mechanical Properties Tests

Mechanical properties tests compressive strength, splitting tensile strength, stress strain curves and modulus of elasticity were carried out. The description of specimen, test equipment and test procedures are discussed under the heading of mechanical properties tests.

3.3.1 Test specimen

The specimens of first class burnt clay bricks with standard dimension of $4\frac{1}{2}$ " x $4\frac{1}{2}$ " x 3" for compressive strength, modulus of elasticity, and stress strain curves were collected from local kiln as shown in Fig 3.1 as per ASTM C 67-14 "Standard Test Methods for Sampling and Testing Brick and Structural Clay Tile." (ASTM C67-14 2014). The dimensions of the bricks were 9" x $4\frac{1}{2}$ " x 3" for splitting tensile strength as shown in Fig 3.2.

The specimens were designated as BBRT, BB200, BB400, BB600 and BB800. The bricks were oven dried in an electric oven to a temperature of 110°C for 24 hours and stored in a cool dry place after that these were engulf into the polythene bags to protect them from the humidity and other environmental effects as shown in Fig 3.3.

3.4 Test Apparatus

Brief description of the test apparatus is presented below.

3.4.1 Splitting Tensile Strength

The splitting tensile strength apparatus consists of (a) Bearing Rods (b) Supplemental Plate and (c) Testing Machine. The bearing rods made up of steel that are matched and paired. The diameter of the rod is of the order of 1/8 to 1/12 of the specimen height and length of the rod is greater than the considered area of the specimen. The thickness of the bearing plate was 1 inch. The plate was fixed in such a manner that it distributes the load uniformly all over the intended surface of the specimen. The testing machine was fulfilling the requirements of Practices E 4. To centrally align the bearing rods with the upper platen of the testing machine a steel circular plate having a diameter of 5 in. and thickness of 1 in. was used. The distance between the upper platen of the testing machine and circular plate was 1/4 in. To determine the splitting tensile strength of BBs, ASTM C 1006 “Standard Test Method for Splitting Tensile Strength of Masonry Units” (ASTM C1006-07 2013) was used as shown in Fig 3.5.

3.4.2 Compressive Strength

Multifunctional Control Console MCC 82 machine used to carry out compressive strength tests as shown in Fig 3.6. It is load controlled test machine. This strength test machine that was utilized to undertake compressive and splitting tensile strength tests is an 1800 kN load controlled compressive test machine which is capable of loading cylinders up to 318 metric tons. To determine the splitting tensile strength of BBs, ASTM C 1314 “Standard Test Method for Compressive Strength of Masonry Prisms” (ASTM C1314-14 2014) was followed.

3.4.3 X-Ray Fluorescence (XRF)

The XRF is done by using the JEOL JSX-3202-M XRF Element Analyzer as shown in Fig 3.7. An accurate and precise determination of metallic and non-metallic elements is done by this machine. The ASTM E 1621 “Standard Guide for Elemental Analysis by Wavelength Dispersive X-Ray Fluorescence Spectrometry” was used for the identification of elements in the specimens. This apparatus consists of mainly five parts (a) Grinder, (b) Pulverizer, (c) Excitation source, (d) Spectrometer and (e) Measuring System.

The grinders are used to produce smooth surface of metals. The pulverizers are used for powders. The excitation source have x-ray tube power supply, providing a stable voltage of sufficient energy to produce secondary radiation from the specimen for the elements specified. The spectrometer is used for x-ray emission analysis and atomic number determination of elements. The measuring system comprises of data output device and pulse height selectors. The data output device can amplify and shape pulses. The pulse height selectors reduce the pulses from high order x-ray lines.

3.4.4 X-ray Powder Diffraction (XRD) Analysis

The x-ray powder diffraction or simply x-ray diffraction (XRD) of burnt masonry bricks (BB) is done on two samples in powdered form a) sample prepared at room temperature (20°C) and b) sample prepared at 800°C temperature. Both the samples were tested at 20 kV voltage and 5 mA current by using 1.54060Å Cu (CuK α) wavelength radiation on STOE Theta-Theta powder diffractometer (© STOE & Cie GmbH). The patterns were scanned in steps of 0.04° in a two angular range from 20° to 80°. The diffractometer generate results in the form of graph. This graph is used to detect the International Center for Diffraction Data number (ICDD) of minerals by using X'Pert High Score software package (X'Pert High Score 1993).

3.4.5 Stress Strain Response

To measure the stress strain response of the BBs a 600 kN load cell and one linear variable displacement transducer (LVDT) was used. These devices were connected to the data logger. It is a real-time data recording instrument. It can measure the load-displacement at a frequency of 4-5 readings per second. To display how much pressure is applied by compressive strength machine to the load cell another instrument called Digimax is used. These instruments are shown in the following Fig 3.12-13.

3.4.6 Electric Furnace

For measuring mechanical properties, the test setup consisted of a temperature controlled electric furnace to heat the specimens up to 800°C. The specimens were exposed to 200°C, 400°C, 600°C and 800°C with a heating rate of 2°C /minute as per RILEM heating standards. The electric furnace was specially designed to simulate high temperature conditions. It is equipped with three components an internal heating electric elements, a ramp and a temperature controller. It is capable of generating different heating rates. The heating chamber consists of 12"×10"×10" in. as shown in Fig 3.12.

3.4.7 Fiberfrax Thermal Insulating Blanket

The heated specimens were carried away from the furnace to the testing machine with the help of a thermal jacket. This thermal jacket was specially designed to minimize the heat loss during transfer of specimen from furnace to the testing machine. This jacket was 2 in. thick and it is made up of refractory ceramic fibers as shown in Fig 3.13.



Fig 3.1: Specimen for ASTM C 1314



Fig 3.2: Specimen for ASTM C 1006



Fig 3.3: Specimen Wrapped in Polythene Bag for ASTM C 1314



Fig 3.4: Specimen Wrapped in Polythene Bag for ASTM C 1314



Fig 3.5: ASTM C 1006 Splitting Tensile Strength Apparatus



Fig 3.6: Multifunctional Control Console MCC 82



Fig 3.7: JEOL JSX-3202-M XRF Element Analyzer

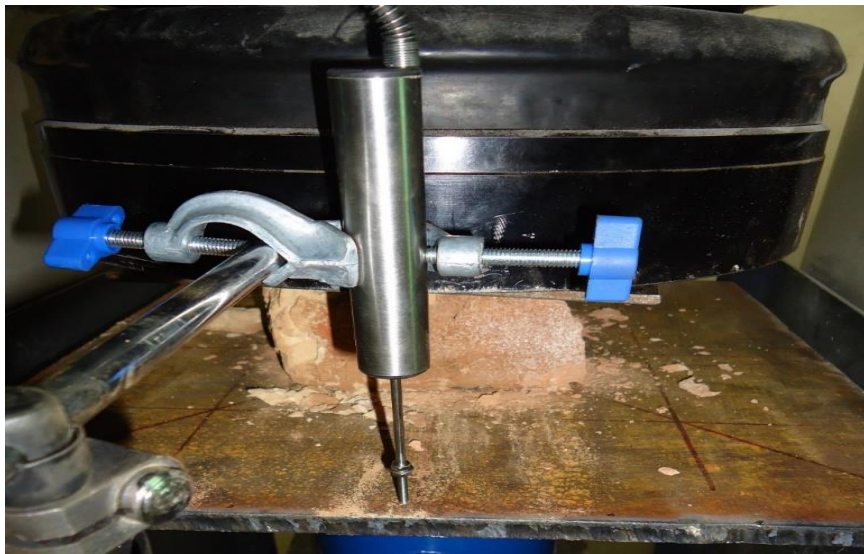


Fig 3.8: LVDT for Measuring Strain



Fig 3.9: Data logger



Fig 3.10: Digimax



Fig 3.11: Load Cell



Fig 3.12: Electric Furnace with Temperature Range up to 800°C



Fig 3.13: Fiberfrax Thermal Insulating Blanket

RESULTS AND DISCUSSION

4.1 General

The evaluated mechanical properties comprising of compressive strength, tensile strength, stress-strain curves and elastic modulus of burnt masonry bricks at elevated temperature are discussed in this section. The x-ray fluorescence (XRF) analysis gives indication of various minerals present in burnt masonry bricks while scanning electron microscopy (SEM) gives visual description of microstructure and porosity of burnt masonry bricks are also demonstrated in this section. Discussion is also presented to compare the mechanical properties of burnt masonry bricks with temperature to that of NSC and HSC.

4.2 Mechanical Properties

4.2.1 Compressive Strength

The bricks were exposed to fire at each target temperature. They were removed from furnace and tested in compression. The recorded applied load at which the heated specimens were failed in compression was used to compute the compressive strength at each temperature. The measured compressive strength of burnt masonry bricks is exhibited in Fig 4.1. It can be seen that from room temperature to 200°C the increase in compressive strength is quite gradual. The following reasons may be responsible for this type of behavior of burnt masonry bricks at 200°C.

The porosity of microstructure plays a significant role in the variation of compressive strength. If the porosity is more the compressive strength will be low. The decrease in porosity increases the compressive strength. When the load is applied slowly to the specimen the fissures or micro-cracks present in the microstructure adjust themselves. The adjustment of these cracks

results in packaging of the microstructure which increase the compressive strength. The release of bound water shrinks the microstructure. This shrinkage densify the microstructure which increases the compressive strength. This release of the bound water causes the mineralogical transformations which alters the lattice of microstructure. As explained earlier the compactness of microstructure increases the compressive strength so the SO_3 from kiln may makes Sulfuric acid during baking of the bricks. This Sulfuric acid stays in the voids of the microstructure.

One possibility of increase in the compressive strength may be baking of partially baked bricks at 200°C for an hour. The Sulfuric acid present in the microstructure of bricks melts after exposure to 200°C . It fills the gap and densify the microstructure. From 200°C to 400°C there is rapid decrease in the compressive strength. This can be attributed to the change in microstructure due to mineralogical transformations of bricks.

From 400°C to 800°C , the compressive strength decreases gradually. From room to 200°C , the increase in compressive strength is minimal with only 3% higher, however when the temperature is further increased to 400°C , the compressive strength is reduced by 46% which can be attributed to mineralogical transformations of bricks. The test data shows that the compressive strength is highest at 200°C with respect to other temperatures. This stabilized behavior of burnt masonry bricks is due to microstructural and mineralogical changes occurred at elevated temperature of 200°C .

The results obtained by different researchers (Andreini and Sassu 2011; Nadjai et al. 2003; Russo and Sciarretta 2013) shows the most unusual trends as compared with test data. The compressive strength increases rapidly from room temperature to 300°C . The compressive strength at 300°C as compared to room temperature is approximately 150% more than that of compressive strength at room temperature this can be attributed to the increase in the content of the bricks aggregate. From 300°C to 500°C the compressive strength decreases but it is still

135% higher than at room temperature as shown in Fig 4.2. There is gradual decrease in compressive strength up to 800°C.

At 800°C only 48% compressive strength is retained. In case of (Andreini and Sassu 2011) there is smooth decline in compressive strength from room temperature to 800°C. At 200°C, 400°C, 600°C and 750°C the compressive strength as compared to room temperature is 90%, 80%, 78% and 75% respectively. In Fig 4.2 it is shown that from room temperature to 400°C the reduction in compressive strength is gradual (Nadjai et al. 2003). The masonry bricks retains 76% of compressive strength.

As the temperature is increased the loss in the compressive strength is rapid. At 800°C 22% of strength remains (Fig 4.2). The results indicate that although there is significant variation in results for compressive strength of burnt masonry bricks at elevated temperatures but overall trend shows a gradual loss of compressive strength.

Results are also presented to compare the fire behavior of burnt masonry bricks to that of NSC and HSC. Fig 4.3 shows the variation of the ratio of residual compressive strength f_c', T at a given temperature to that at room temperature for HSC and NSC except for burnt masonry bricks (BB) actual or real time compressive strength f_c', T at a given temperature to that at room temperature. The HSC and NSC show similar behavior of strength loss at elevated temperatures. The compressive strength of both concrete types and burn clay bricks decreases with temperature.

At 400°C the HSC (Fu et al. 2005), NSC (Fu et al. 2004; Tang and Lo 2009) shows retention in compressive strength. While the compressive strength value reported by (Khaliq and Kodur 2012) and test results show much loss in compressive strength (Fig 4.3). At 200°C the compressive strength of burnt masonry bricks is found to be higher than NSC and HSC. This can be attributed to the mineralogical transformations and microstructural improvement in

burnt masonry bricks at that temperature. In Fig 4.3 it is shown that from 200°C to 400°C the decrease in compressive strength is rapid as compared to NSC and HSC (Fu et al. 2004; Fu et al. 2005; Tang and Lo 2009). The strength loss follows the similar trends in these materials. The overall behavior is similar to that of NSC and HSC.

4.2.2 Tensile Strength

The comparison of tensile strength of burnt masonry bricks with other researchers is shown in Fig 4.4. The measured splitting tensile strength of burnt masonry bricks is illustrated in Fig 4.4. The splitting tensile strength of burnt clay brick shows peak value at 200°C. From room temperature to 200°C the tensile strength is rapidly increased. As the temperature is further increased there is rapid decrease in tensile strength up to 400°C. There is gradual decrease in the tensile strength from 400°C to 800°C.

There is not much data on tensile strength of burnt masonry bricks in literature, however the behavior of test data on burnt masonry bricks is compared with that of NSC and HSC.

The tensile strength of masonry as a function of temperature is labelled in Fig 4.5. The tensile strength decreases as temperature is increased (Nadjai et al. 2003; Xiao et al. 2013) and test data as depicted in Fig 4.5. (Nadjai et al. 2003) found that the decrease in tensile strength from room temperature to 400°C is gradual but as the temperature is further increased the reduction is very smooth. Only 10% of tensile strength is retained at 800°C.

All tensile strength is lost at 1000°C. The trend shown by (Xiao et al. 2013) and test data is almost similar except at 200°C. The tensile strength calculated by (Xiao et al. 2013) shows much retention at 300°C i.e., only 2% strength is lost. Up to 500° 50% strength is lost. From 500°C to 800°C there is slow decrease in tensile strength. Only 1% tensile strength is holding by samples.

The peak point at 200°C of tensile strength of the test data is eye catching because the sheer increase in the strength value is not following the current trend. Irrespective of the decrease in tensile strength, it increases (Fig 4.6). At 200°C it more than 400% strength is gained. Although further increase in temperature decreases the strength in a similar way as it is increased but it is still 250% more as compared to room temperature.

When the 600°C temperature is achieved the tensile strength is lost as compared to the strength at 400°C but 200% strength is achieved. Same trend is followed up to 800°C but the tensile strength is still more than 140% to that of room temperature. The abrupt behavior of test data can be attributed to the fact that these strength values are obtained at real time elevated temperature.

The Fig 46 exhibits the comparison of tensile strength of NSC, HSC and burnt masonry bricks. The tensile strength loss trend shows that the burnt masonry bricks attain tensile strength at 200°C than loose it gradually with increase in temperature while the tensile strength loss in NSC and HSC is uniform throughout the temperature range of 20°C-800°C. The comparison shows that the tensile strength loss trend of burnt masonry bricks are not similar to that of NSC and HSC.

The tensile strength is very important property for HSC and NSC regarding propagation of cracks. In the event of fire the tensile strength decreases drastically. The tensile strength is crucial where the fire induced spalling is the governing factor (Fig 46). The tensile strength of NSC is higher than HSC due to its less dense microstructure. The bound water evaporates through porous structure of NSC while in HSC it erupts the concrete surface thereby decreasing the tensile strength of it.

4.2.3 Stress Strain Curves

The load and deformation data generated from compressive strength tests was used to compute stress strain response of BBs in temperature range of 20 to 800°C. The stress strain curves shown in Fig 4.7 for BBs can be distinctively divided into three segments at all temperatures. First segment shows ductile response with higher strains at low stresses in the range of about 6-7% strains. The second segment shows almost linear response up to peak stress with much stiff behavior of BBs and the corresponding increase in strain is lower as compared to first segment.

This can be attributed to the initial microstructural adjustments under load due cracks and porosity present in samples (Watstein 1971). The third segment is from peak stress to failure stress (ultimate strain) where large deformations occur at reduced stresses. Overall, the response of stress-strain curves at each target temperature follows similar trend. The response of BBs varies from ductile at initial phase to stiff and then again to ductile behavior and confirmed as attained and presented by Mbumbia and de Wilmars (2002).

As the major part of stress strain curves is stiff, it can be deduced that overall, the response of BBs is brittle, however, the post peak behavior becomes slightly ductile. From room temperature to 800°C, there is an increase in the peak strain of 28%, 44%, 74% and 91% at 200, 400, 600 and 800°C temperatures respectively. On the other hand, from 200-800°C the corresponding stress decreases by 94%, 87%, 80% and 66% respectively corresponding to that at room temperature. It can also be observed from Fig 4.7 that the post peak response at each target temperature follows almost same slope, therefore it is believed that BBs have quite stable behavior before failure. The initial part of ductile response can be attributed to the readjustment of flaky and crystalline microstructure of BBs, where perforations in crystals adjust under load.

The stiff response then is attained by interlocking and new adjusted microstructure which takes more stress and allows less increase in strains.

From Fig 4.7 it can be postulated that from room temperature to 800°C the gradient of curves decreases gradually and there is increase in the non-linear behavior of the masonry bricks as the temperature is increased which can be attributed to the changes in microstructure due to increase in the width of micro cracks, pores and fissures as the temperature is increased (Mbumbia and de Wilmars 2002).

The stress strain curve of burnt masonry brick obtained at 200°C shows lower values of stress but higher values of strain as compared to values at 20°C. After peak point of 4.7 MPa the curve becomes almost straight until failure occurs at 4.6 MPa which can be attributed to the propagation of micro cracks.

The curve obtained at 400°C shows peak value of stress of 4.3 MPa with a corresponding strain of 0.17. There is similar trend of curve as that of 200°C up to stress level of 1.5 MPa. There is increase in the stress up to peak value of 4.3 MPa which can be attributed to the initiation of transformation of Kaolinite. The peak value of strain in case of stress strain curve obtained at 600°C is 4 MPa while failure strain is 0.22 (mm/mm) which can be attributed to the Metakaolinite which has amorphous structure. The lowest values of stresses and corresponding higher strain values are obtained at 800°C.

First portion of strains ends at 7% of strain values and the other straight portion ends 0.18% strain values with a corresponding stress of 2.5 MPa. The stiff response at 800°C is obtained only between 0.18 and 0.2% strain values with a corresponding maximum stress values of 3.3 MPa.

4.2.4 Elastic Modulus

The comparison of elastic modulus of burnt masonry bricks at elevated temperatures is shown in Fig 4.9. The test data shows that there is considerable variation in elastic modulus from room temperature to 800°C as shown in Fig 4.9. At 200°C the value of elastic modulus is lowest. The reduction in elastic modulus is significant from room temperature to 200°C. There is 50% retention of elastic modulus at temperature of 400°C. From 400°C to 600°C there is very minor decrease in the elastic modulus. There 75% reduction in elastic modulus at 800°C as compared to room temperature.

The comparison of relative tangent elastic modulus of BBs in hot state to residual conditions with various researchers (Andreini and Sassu 2011; Russo and Sciarretta 2013) at elevated temperatures is shown in Fig 4.10. The trend in decrease of elastic modulus is same with the increase in temperature. The elastic modulus values of test data are 9.3% lower than Andreini and Sassu (2011) and 6.2% higher than Russo and Sciarretta (2013) up to 200°C temperature. At 400°C the test data gives modulus similar to Andreini and Sassu (2011) but elastic modulus values of Russo and Sciarretta (2013) are 17.6% lower than test data as can be seen in Fig 4.10. From 400°C to 800°C obtained modulus values for BBs are lower than both (Andreini and Sassu 2011) and (Russo and Sciarretta 2012). This difference in modulus behavior can be attributed to hot and residual behavior of BBs and also to changes in microstructure at elevated temperatures.

The comparison of relative elastic modulus of BBs compared to that NSC and at various temperatures is shown in Fig 4.11. There is no consistent pattern of decline of modulus but the overall pattern shows that the loss is similar to NSC and HSC with increase in temperature. The loss of modulus is more consistent in comparison to NSC as it shows (Fig 4.11) almost similar trend observed by other researchers (Ayala 2011; Bažant 1996; Phan 2000). However, as shown in Fig 4.11, loss of modulus is higher in BBs compared to HSC especially in 20-

400°C. Beyond 400°C the loss almost follows trend of loss in elastic modulus in HSC as reported by various researchers (Castillo and DurraniI 1990; Khaliq 2012; Phan 1996). The difference in decrease of modulus can be attributed to the basic difference in BBs and that of HSC, where breakage of bonds in microstructure of cement paste and disintegration of cement hydrated products, type of aggregates and high temperature creep are responsible factors for degradation in modulus of HSC at elevated temperatures.

There is no regular pattern of decline of elastic modulus as we can see from room temperature to 400°C and 600°C to 650°C the decrease in elastic modulus is rapid. The decrease in elastic modulus is smooth from 200°C to 400°C and from 650°C to 800°C. At 400°C the elastic modulus value is 60% to that of room temperature. An elastic modulus loss of 83% is observed at 650°C. Another research indicate that there is gradual fall in elastic modulus values as predicted by (Andreini and Sassu 2011) from 200°C to 800°C but there is speedy decrease in elastic modulus of 40%, up to 200°C. The elastic modulus values obtained by (Bažant 1996) indicate that up to 400°C the decrease in the elastic modulus is gradual. The elastic modulus is retained 43% at 400°C. The elastic modulus value decreases more gradually up to 800°C.

The comparison of loss in elastic modulus of burnt masonry bricks with that of NSC and HSC is illustrated in Fig 2.15. The fire resistance of structural members is influenced by the decrease in the elastic modulus of HSC at elevated temperatures. The breakage of bonds in microstructure of cement paste and disintegration of cement hydrated products, type of aggregates and high temperature creep are responsible factors of elastic modulus degradation at elevated temperatures.

The variation of the ratio of elastic modulus at the target temperature to that at room temperature is shown in Fig 2.15 the reduction in elastic modulus of HSC reported by (Castillo and Durrani 1990; Khaliq and Kodur 2012; Phan 1996) shows similar trend of reduction in elastic modulus at elevated temperature but the variation in reported data is significant.

4.3 X-Ray Fluorescence (XRF) Analysis

The mass percentages of elements from room temperature to 800°C do not show significant variation as shown in Fig 4.13. The Iron (Fe) element is present in abundance among all elements present in clay bricks. At 200°C the mass percentage of Iron (Fe) shows significant reduction. At the same temperature the copper (Cu) is also abundantly present. Among all the temperatures, the temperature of 200°C shows less amount of mass percentage of all elements present in burnt clay brick. At room temperature, the burnt clay brick have highest quantity of Calcium (Ca). At 600°C the Iron (Fe) content is the second largest element present. The temperature of 600°C and 800°C shows similar element content of Potassium (K), Calcium (Ca), Titanium (Ti) and Iron (Fe). The Manganese (Mn), Strontium (Sr), Zirconium (Zr) and Zinc (Zn) are present only in traces (Fig 4.13).

The compressive strength of bricks made from waste slag does not show any sintering behavior up to 800°C which is the ultimate firing temperature for test data. Above 950°C the sintering behavior continues which cause increase in the compressive strength. there are no crystal change At 200°C the Potassium (K), Calcium (Ca) and Iron (Fe) content is lowest as compared to their content at other temperatures. The increase in the mechanical properties at 200°C may be due to the decrease in the porosity which densify the microstructure.

The closing of microscopic fissures and sharp notches present in the microstructure under the action of slow loading may be responsible for increase in the mechanical strength at 200°C. The very low content of Silica (SiO₂) is responsible for low plasticity which impart

heterogeneities and result in weak microstructure which decreases the mechanical strength (Mbumbia and de Wilmars 2002). The mineralogical transformations and release of bound water from the minerals makes the microstructure dense (Klosek-Wawrzyna et al. 2013). The bricks may be under burnt, when they are exposed to fire at 200°C for about an hour the Sulfuric acid which is produced because of the SO₃ from kiln dissolves the Potassium (K), Sodium (Na) and Magnesium (Mg) minerals and result in the formation of glassy phase. This glassy phase reduces the porosity and thus responsible for the increase in the mechanical strength at 200°C (Brownell 2012; Mezenchevova et al. 2012).

The increase in the mechanical resistance at 200°C can be attributed to the reduction in the Calcite (CaCO₃) and Portlandite (Ca(OH)₂) phases (El-Mahllawy and Kandeel 2014) There are no significant mineralogical transformations occurred in the temperature range of room temperature to 800°C (Fig 4.13). The further decrease in the mechanical resistance at 400°C, 600°C and 800°C is attributed to the presence of pores, fissures and micro-cracks in the microstructure of the bricks. (Paterson and Wong 2005).

The mineralogical transformations continue at 400°C which results in the decrease in volume of minerals as shown in Fig 4.13. From 450°C to 950°C the kaolinite is converts into meta-kaolinite the porosity increase and relative strength properties also decreases (Hachemi and Ounis 2014) the crystallinity of kaolinite started to decrease above 400°C. The XRF analysis shows that the Calcium (Ca) content is more than that at 200°C as compared to other temperatures. This element is the key component of Carbonate. The Carbonate increase absorption and interconnection of pores and makes less dense the microstructure which lowers the mechanical strength.

4.4 X-ray Powder Diffraction (XRD) Analysis

The XRD pattern of sample at 20°C temperature is shown in Fig 4.14. The most abundant minerals present in BB with their reference code, name and formula are tabulated in Table 4.3. The minerals present in abundance at peaks in Fig 4.14 are Halite, Feldspar, Mullite, Hematite, Kaolinite, Muscovite, Orthoclase and Montmorillonite. At 800°C, Albite mineral appeared in peaks but Feldspar and Hematite disappeared at peaks (Fig 4.15) when compared with Fig 4.14. At 20°C 14 minerals were detected (Table 4.3) whereas at 800°C 18 minerals were found (Table 4.4). Additionally, at 800°C presence of Lime, Magnesia and Potassium Aluminum Silicate were also measured with respect to 20°C temperature. The Chlorite Ion (ICDD 01-079-2398) when treated with heavy metals they decompose when heated was displayed by XRF analysis as shown in Fig 4.13. The heating process may cause reaction of this ion with heavy metals and cause decomposition of microstructure when heated to 800°C temperature (Greenwood N.N. and Earnshaw A. 2006). The Calcite (ICDD 00-047-1743) when heated to above 400°C temperature transforms into Vaterite which is less stable polymorph of Calcium Carbonate. This may have led to decrease in the mechanical properties of BB at elevated temperatures (Yoshioka S. and Kitano Y. 1985). Illite (ICDD 00-026-0911) has layered prismatic structure when heated it converts into Muscovite (ICDD 00-001-1098) (Gharrabi M. et al. 1998). This might also lead to decrease in mechanical properties of prismatic structures is broken at service loads if exposed to elevated temperatures. The dehydration of Kaolinite (ICDD 01-075-0938) is completed around 150°C and its dehydroxylation occurs between 500-600°C temperature range. The structural breakdown occurs between 800-900°C which may cause decrease in mechanical properties of BB at elevated temperatures (McConville C.J. and Lee W.E. 2005).

There is difference in mineral phases at 20°C and 800°C. These different phases may be responsible for the decrease in mechanical properties at elevated temperatures. The firing transformations, presence of fissures and development of micro cracks when load is applied can be the prominent factors in decreasing the mechanical performance of BB at elevated temperatures (McConville C.J. et al. 1998). Overall the clays may be thermally converted into other phases when baked at elevated temperatures, the structurally bound water in minerals is evaporated thus transforming the minerals into different phases at elevated temperatures (Lee S. et al. 2001).

4.5 Microscopic Study of Surface Texture

At different temperatures the mineralogical composition is minutely altered and this alteration in quantity of minerals is not significant. From room temperature to 800°C the microstructure evolve from grains to somehow irregular flaky particles. At room temperature the SEM micrographs shows granular structure when the temperature is increased to 200°C the Sulfuric acid liquefies and fills the pores and granular structure merges and turns into flaky particles. These flaky particles join together to fill the gap within microstructure thus increasing the mechanical strength at 200°C (Brownell 2012; Mezencevova et al. 2012) as can be seen in Fig 4.14 at the resolution of 5 μm .

At 400°C the flaky particles again turn into granular structure but the grain size is greater than which is present at room temperature and creates empty spaces makes structure less dense as depicted in Fig 4.14 at the resolution of 10 μm . Particularly at 600°C the microstructure becomes porous as compared to all other temperatures. The flaky particles which were present at 600°C are now turned again into smaller grains (Seynou et al. 2011). At 800°C the glassy phase dominate the liquid phase the pores sizes increases. Porous glassy microstructure breaks

abruptly when the load applied on it. This behavior responsible for the rapid decrease in the strength at 800°C and can be clearly seen in Fig 4.14 at zooming level of 10 μm.

4.6 High Temperature Material Property Relationships for Burnt Masonry Bricks

The material properties measured at elevated temperatures give physical constants in the form of mathematical equations that can be used as mathematical models for the fire resistance calculations of structures made of BBs. The use of such equations facilitates the application of these mathematical models for the calculation of fire resistance ratings of such structures (Lie 1992). These material properties are expressed in the form of empirical relations over temperature range of 20-800°C in the form of empirical relations for compressive strength, splitting tensile strength, elastic modulus, and compressive toughness of bricks. These relations are arrived at by using linear regression analysis on mechanical properties obtained through test results. For regression analysis, measured material properties were used as a dependent variable with temperature as their independent variable.

The least-squares procedure is used for fitting a line through a set of ‘n’ data points where it is desired that the differences between the observed values and corresponding points on the fitted line should be minimum. A convenient way to accomplish this, and one that yields estimators with good properties, is to minimize the sum of squares of the standard deviations from the fitted line. In this case the deviations are actually the errors in the values of material properties (dependent variable) given by the values of temperatures (independent variables) and to reduce these deviations in the dependent values sum of the square of error is utilized.

Commercial software, Minitab (Minitab 2013) was used to carry out the regression analysis of the material properties obtained from experimental results. For regression analysis, coefficient of determination R^2 was evaluated to define the accuracy of the best fit equation (Wackerly et al. 2008). This R^2 is actually the proportion of total variation in the response that is explained

by the variable prediction in a simple regression model and represents the proportion of the sum of square of error about their independent variable.

The values of coefficient determination R^2 obtained for material property equations for masonry bricks at elevated temperatures lie between 0.99-1, which represents a reasonably high confidence level in on proposed equations.

The relationships for compressive strength, splitting tensile strength, elastic modulus and compressive toughness are tabulated as $\beta_{T, compressive}$, $\beta_{T, tensile}$, $\beta_{T, modulus}$, and $\beta_{T, toughness}$ in Table 4.1 respectively. In lieu of equations as presented in Table 4.1, the values of these coefficients (β_T) can also be used for evaluating the compressive and tensile strength, elastic modulus, and compressive toughness at a certain elevated temperature for burnt masonry brick as tabulated in Table 4.2.

Table 4.1: High Temperature unstressed material property relationship for burnt masonry bricks

Material Property		Relation
Compressive strength	$\beta_{T, compressive}$	$\left\{ \begin{array}{ll} 1.0 & 20^{\circ}\text{C} \\ 1.39 - 0.0015T & 20^{\circ}\text{C} < T \leq 800^{\circ}\text{C} \end{array} \right\}$
Splitting Tensile strength	$\beta_{T, tensile}$	$\left\{ \begin{array}{ll} 1.0 & 20^{\circ}\text{C} \\ 0.9942 + 0.0002T & 20^{\circ}\text{C} < T \leq 200^{\circ}\text{C} \\ 1.4402 - 0.0018T & 200^{\circ}\text{C} < T \leq 800^{\circ}\text{C} \end{array} \right\}$
Elastic Modulus	$\beta_{T, modulus}$	$\left\{ \begin{array}{ll} 1.0 & 20^{\circ}\text{C} \\ 1.0468 - 0.002T & 20^{\circ}\text{C} < T \leq 200^{\circ}\text{C} \\ 0.8257 - 0.0008T & 200^{\circ}\text{C} < T \leq 800^{\circ}\text{C} \end{array} \right\}$
Compressive Toughness	$\beta_{T, toughness}$	$\left\{ \begin{array}{ll} 1.0 & 20^{\circ}\text{C} \\ 0.9912 + 0.0014T & 20^{\circ}\text{C} < T \leq 600^{\circ}\text{C} \\ 3.0264 - 0.002T & 600^{\circ}\text{C} < T \leq 800^{\circ}\text{C} \end{array} \right\}$

Table 4.2: Compressive strength, tensile strength, elastic modulus, and compressive toughness reduction factors (β_T) at different temperatures for burnt masonry bricks

Reduction Factor (β_T)				
Temperature (°C)	Compressive Strength ($f'_{c,T}$)	Splitting Tensile Strength ($f'_{t,T}$)	Elastic Modulus (E,T)	Compressive Toughness ($T_{c,T}$)
20	1	1	1	1
200	0.95	1.03	0.65	1.31
400	0.87	0.72	0.51	1.55
600	0.79	0.36	0.35	1.83
800	0.71	0	0.19	1.44

Table 4.3: Minerals name, composition and reference code present in BB at 20°C temperature

Serial No.	Reference Code	Mineral Name	Chemical Formula
1	01-079-2398	Chlorite	ClO_2^-
2	00-047-1743	Calcite	$CaCO_3$
3	01-070-0909	Gypsum	$CaSO_4$
4	01-080-1027	Pyrite	FeS_2
5	01-089-8575	Feldspar	$KAlSi_3O_8 - NaAlSi_3O_8$ $-CaAl_2Si_2O_8$ (K, H_3O)
6	00-026-0911	Illite	$Al_2Si_3AlO_{10}(OH)_2$
7	00-013-0259	Montmorillonite	$(Na, Ca)_{0.33}(Al, Mg)_2(Si_4O_{10})$
8	01-089-3615	Halite	$NaCl$
9	00-043-0596	Quartz	SiO_2
10	01-075-0938	Kaolinite	$Al_2Si_2O_5(OH)_4$
11	01-076-0749	Orthoclase	$KAlSi_3O_8$
12	01-088-2359	Hematite	Fe_2O_3
13	00-001-1098	Muscovite	$KAl_2(AlSi_3O_{10})(F, OH)_2$
14	01-088-2049	Mullite	$Al_6Si_2O_{13}$

Table 4.4: Minerals name, composition and reference code present in BB at 800°C temperature

Serial No.	Reference Code	Mineral Name	Chemical Formula
1	01-079-2398	Chlorite	ClO_2^-
2	00-047-1743	Calcite	$CaCO_3$
3	01-070-0909	Gypsum	$CaSO_4$
4	01-080-1027	Pyrite	FeS_2
5	01-089-8575	Feldspar	$KAlSi_3O_8 - NaAlSi_3O_8$ $-CaAl_2Si_2O_8$ (K, H_3O)
6	00-026-0911	Illite	$Al_2Si_3AlO_{10}(OH)_2$
7	00-013-0259	Montmorillonite	$(Na, Ca)_{0.33}(Al, Mg)_2(Si_4O_{10})$
8	01-089-3615	Halite	$NaCl$
9	00-043-0596	Quartz	SiO_2
10	01-075-0938	Kaolinite	$Al_2Si_2O_5(OH)_4$
11	01-076-0749	Orthoclase	$KAlSi_3O_8$
12	01-088-2359	Hematite	Fe_2O_3
13	00-001-1098	Muscovite	$KAl_2(AlSi_3O_{10})(F, OH)_2$
14	01-088-2049	Mullite	$Al_6Si_2O_{13}$
15	00-030-0794	Magnesia	MgO
16	01-076-0898	Albite	$NaAlSi_3O_8$
17	00-050-0008	Lime	$Ca(OH)_2$
18	00-026-0895	Potassium Aluminum Silicate	$KAl_2(AlSi_3O_{10})(OH)_2$

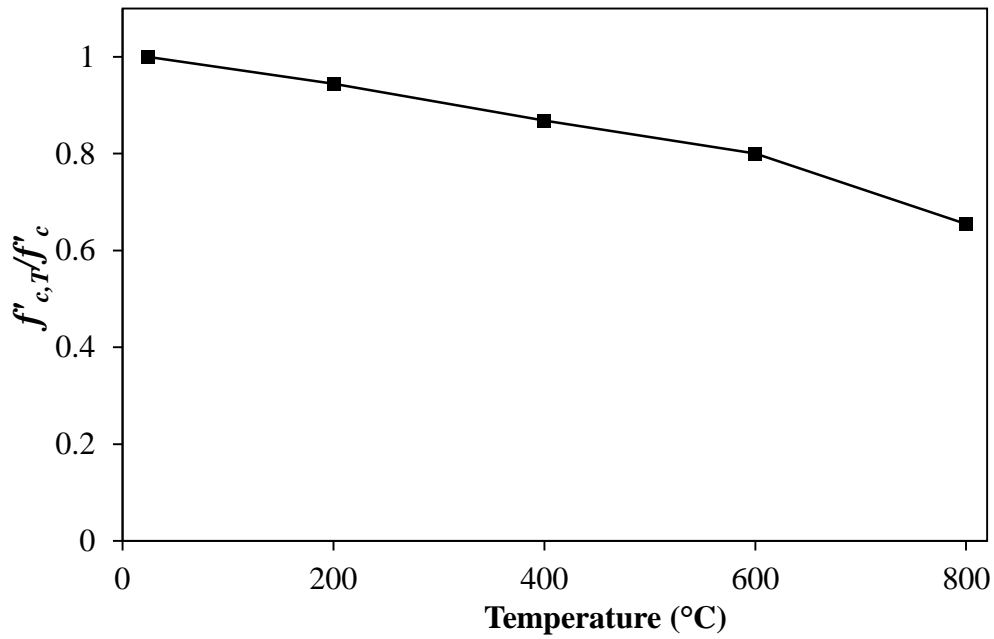


Fig 4.1: Variation in relative compressive strength of burnt masonry bricks (Test Data) as a function of temperature

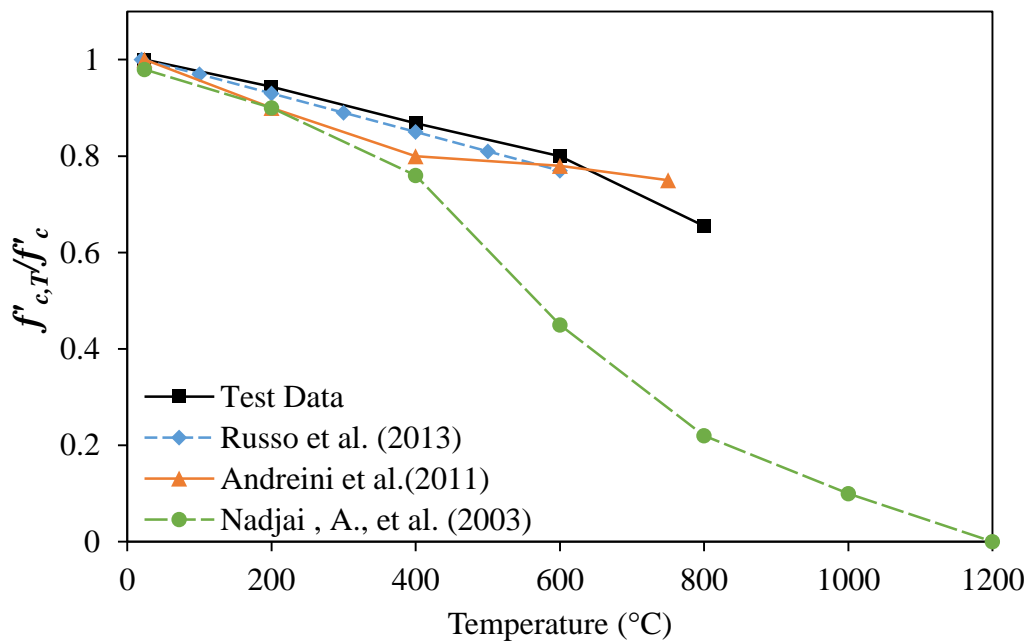


Fig 4.2: Comparison of variation in relative compressive strength of burnt masonry bricks as a function of temperature

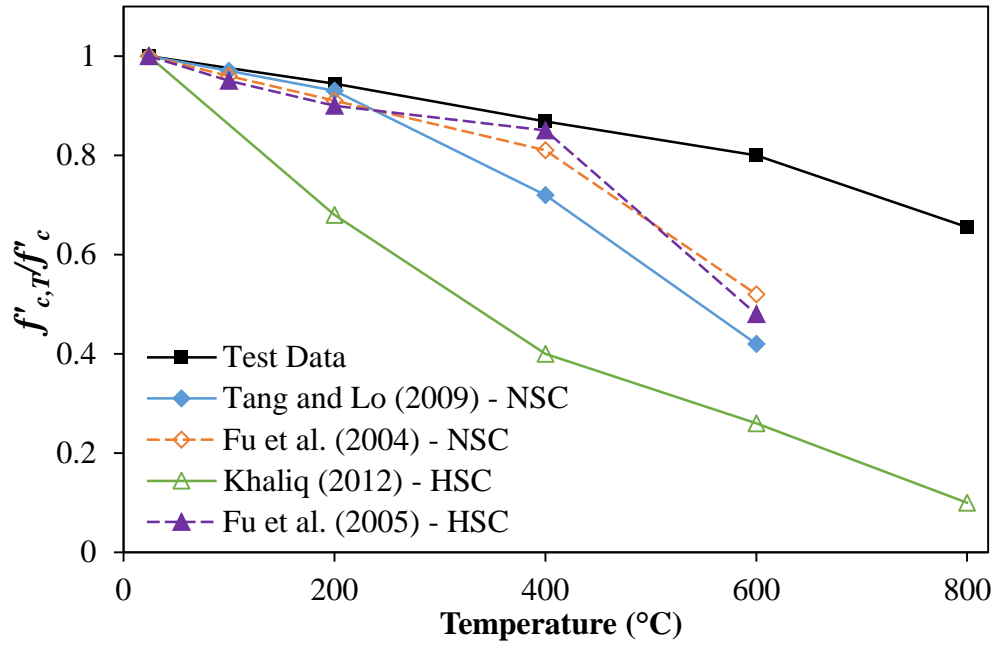


Fig 4.3: Relative compressive strength of HSC, NSC and burnt masonry bricks as a function of temperature

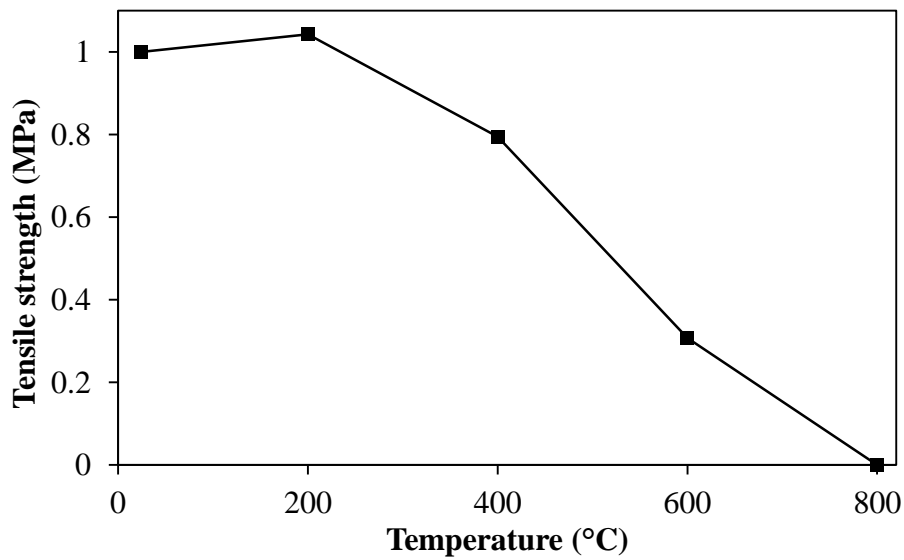


Fig 4.4: Relative tensile strength of burnt masonry bricks as a function of temperature

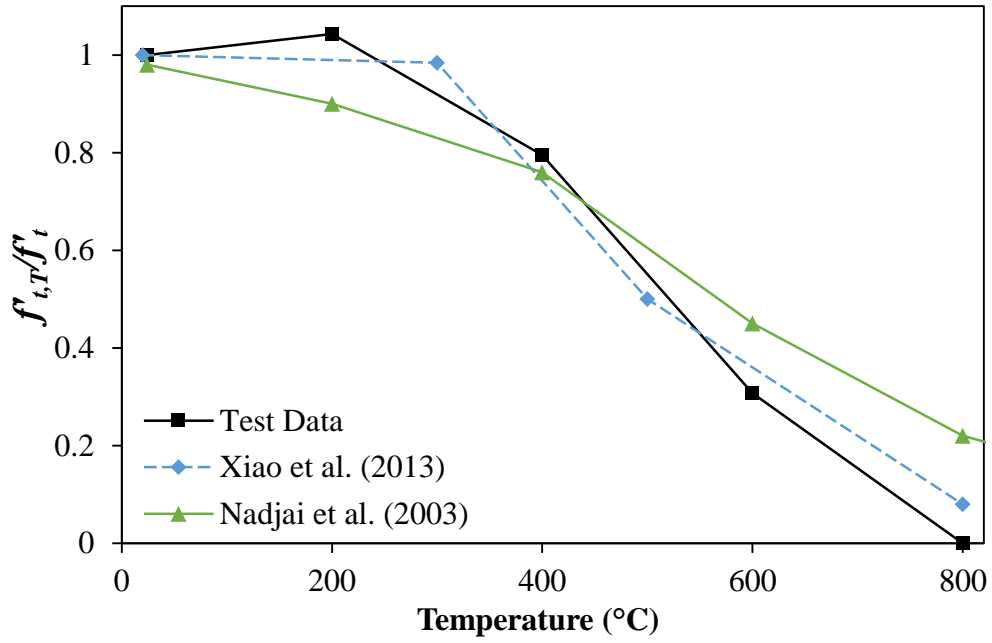


Fig 4.5: Comparison of variation in relative tensile strength of burnt masonry bricks as a function of temperature

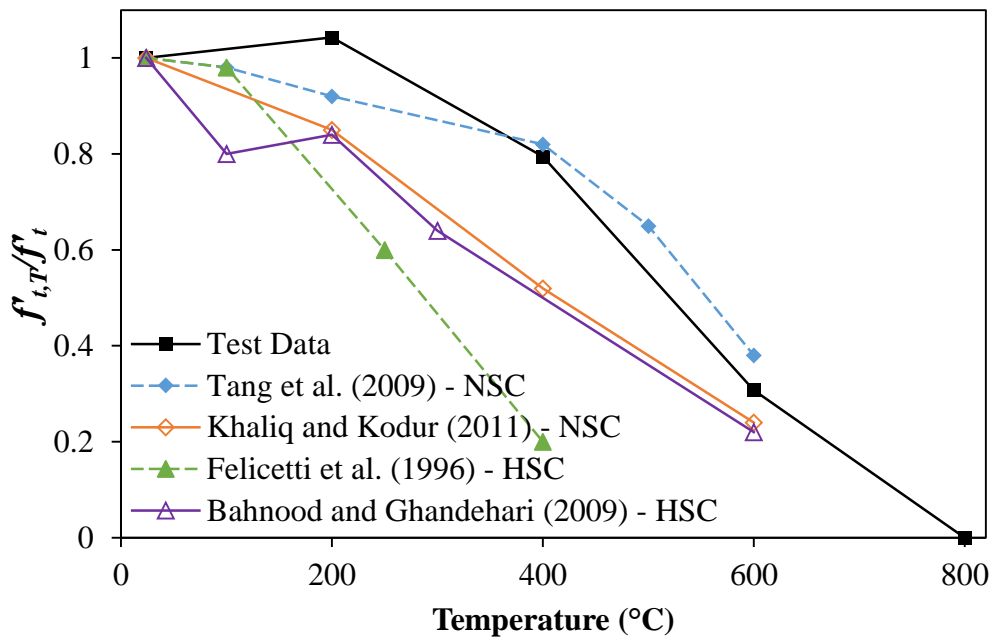


Fig 4.6: Variation in relative tensile strength of HSC, NSC and burnt masonry bricks (BB) as a function of temperature

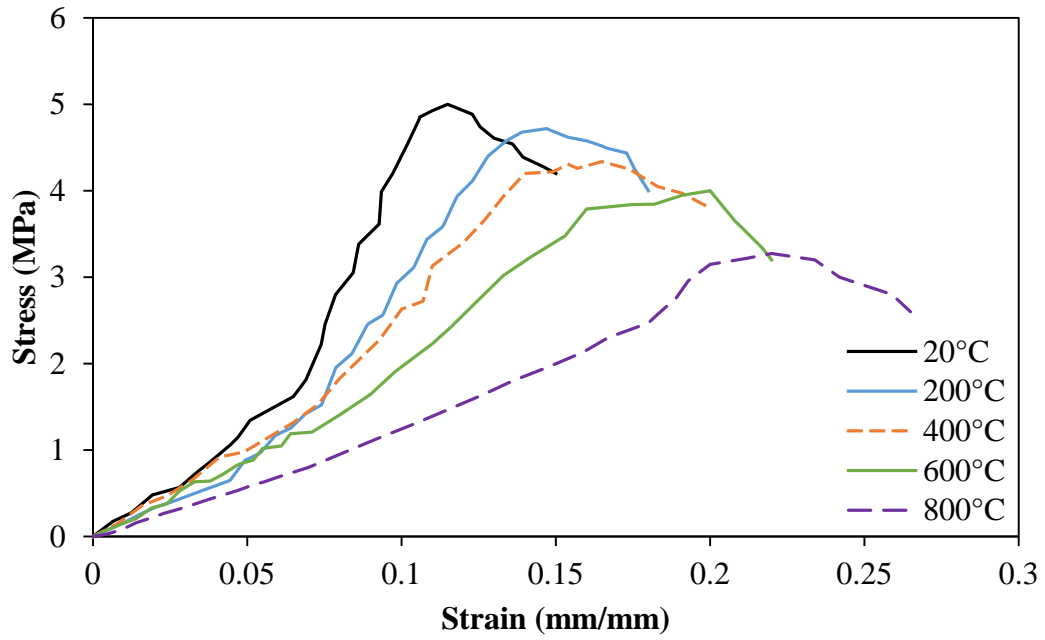


Fig 4.7: High temperature stress strain curves of burnt masonry bricks

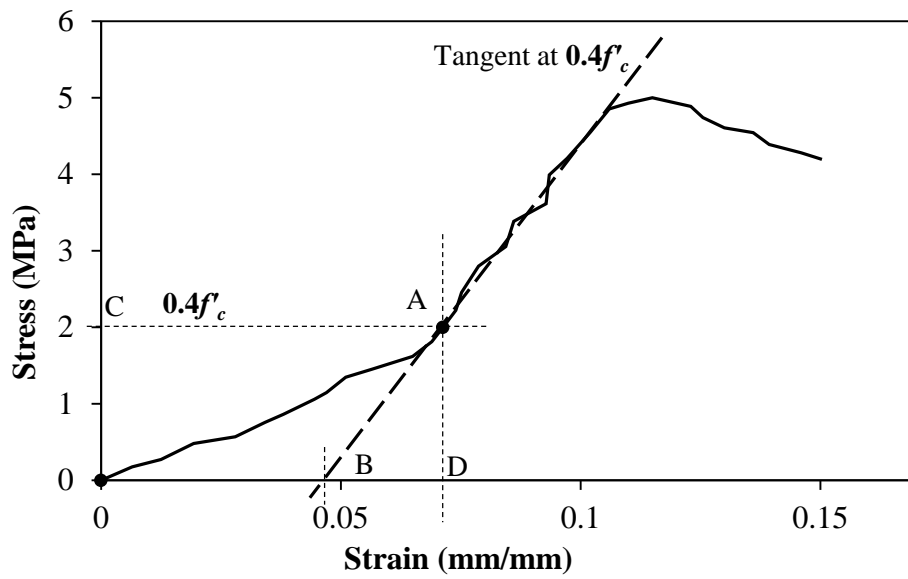


Fig 4.8: High temperature stress strain curves of burnt masonry bricks

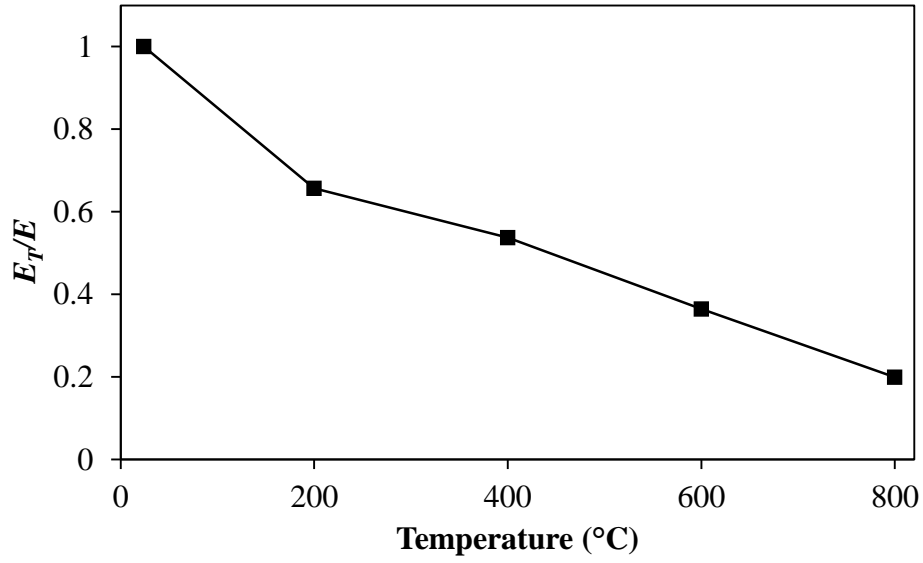


Fig 4.9: Relative elastic modulus of burnt masonry bricks as a function of temperature

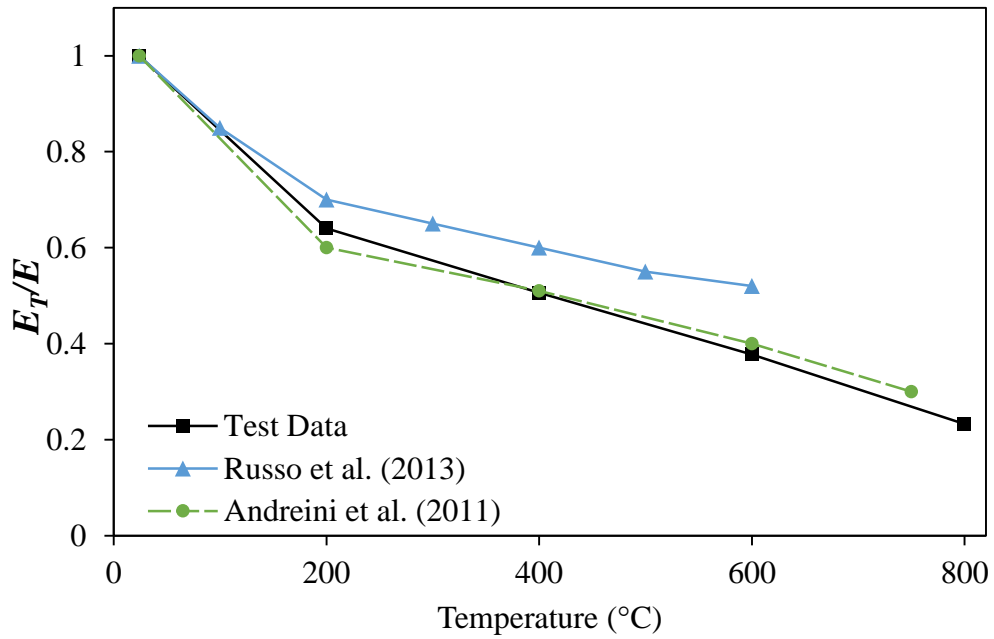


Fig 4.10: Variation in relative elastic modulus of burnt masonry bricks as a function of temperature

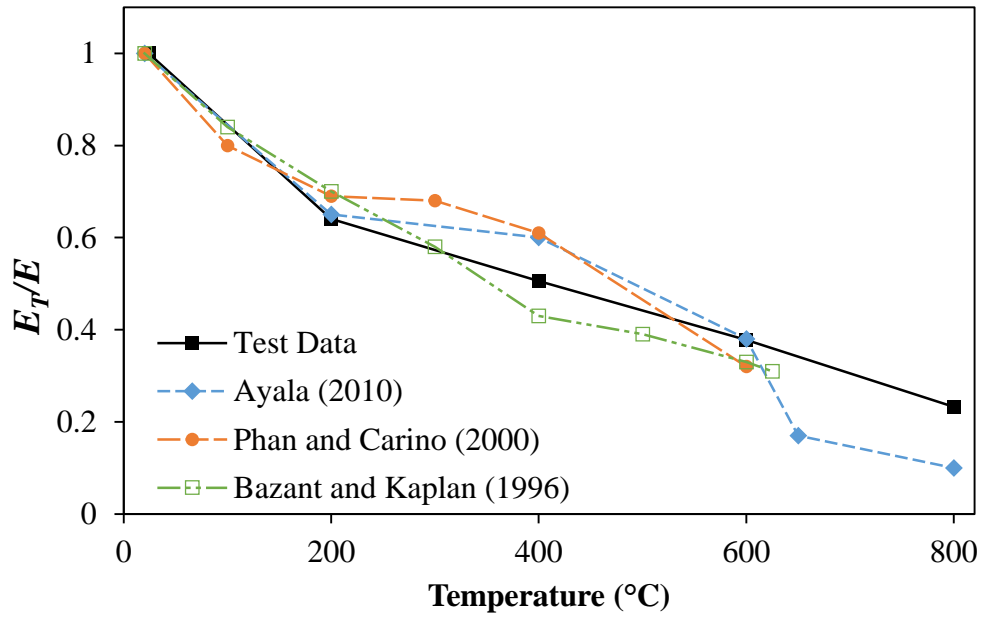


Fig 4.11: Variation in relative elastic modulus of burnt masonry bricks as compared to NSC at elevated temperatures

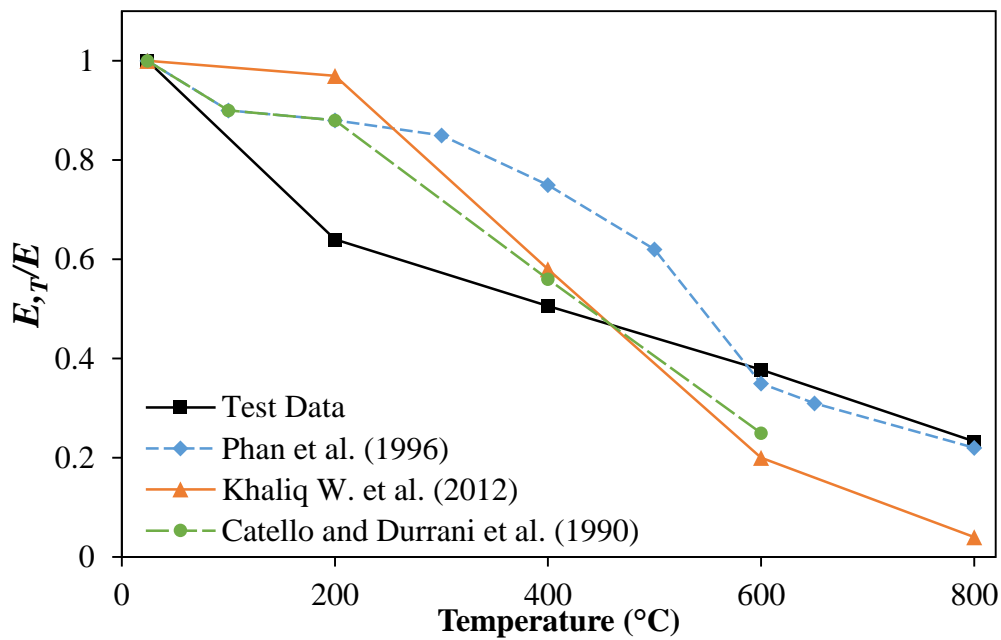


Fig 4.12: Variation in relative elastic modulus of burnt masonry bricks as compared to HSC at elevated temperatures

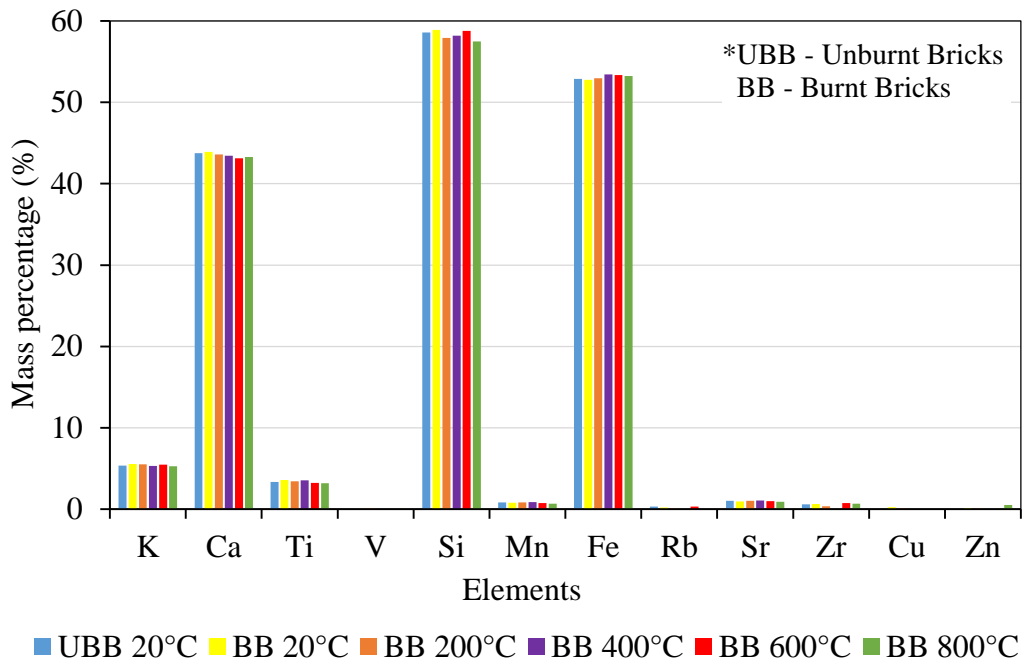


Fig 4.13: XRF of burnt masonry bricks at different temperatures

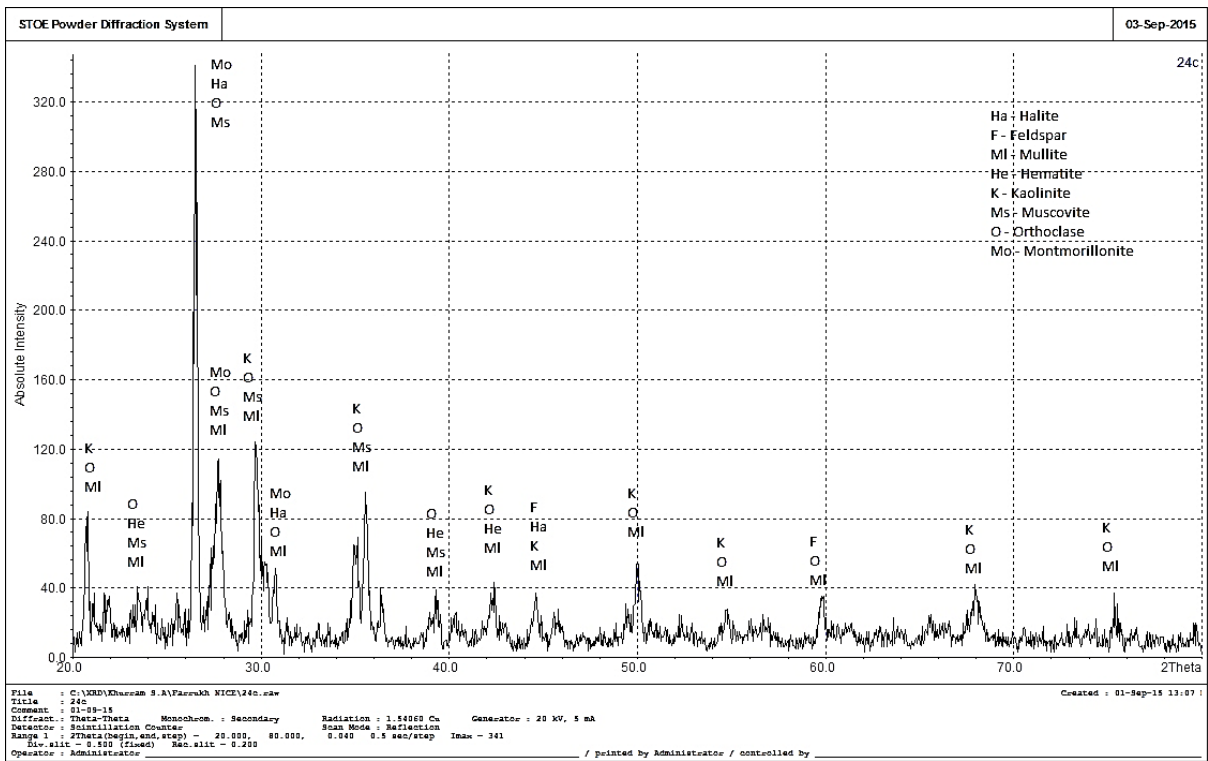


Fig 4.14: XRD diffraction analysis of BB at 20°C temperature

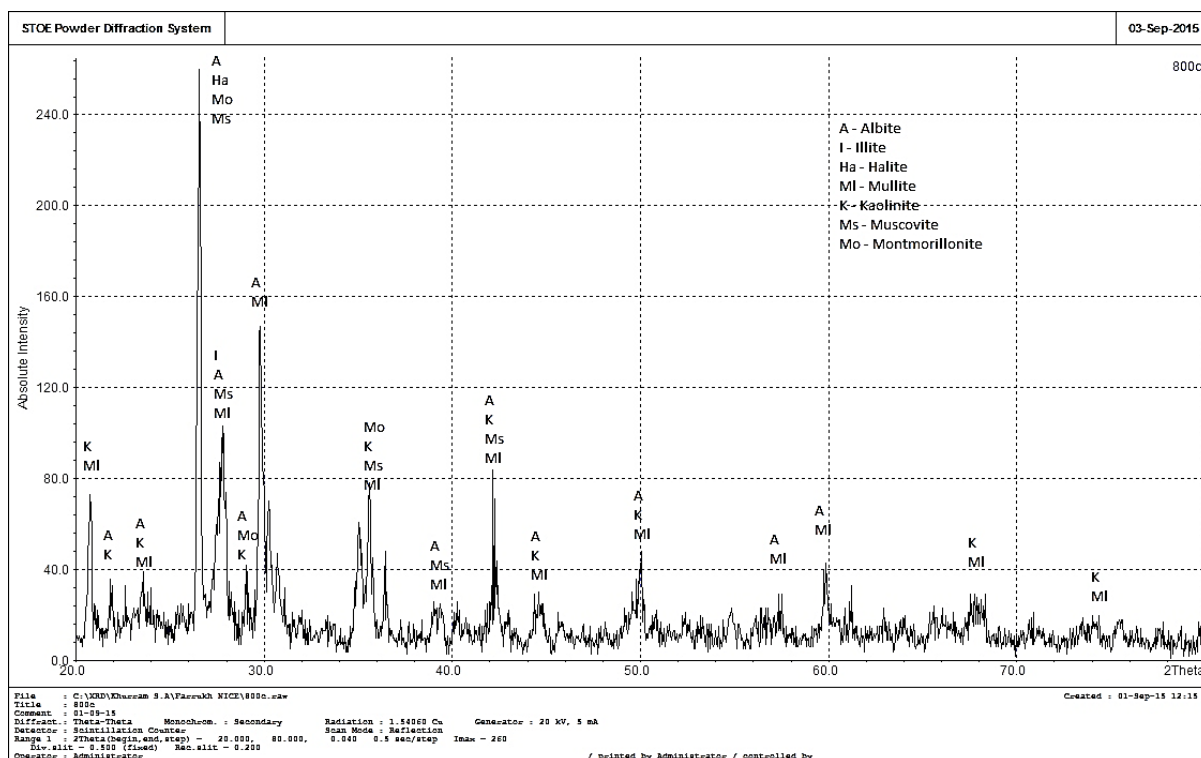


Fig 4.15: XRD diffraction analysis of BB at 800°C temperature

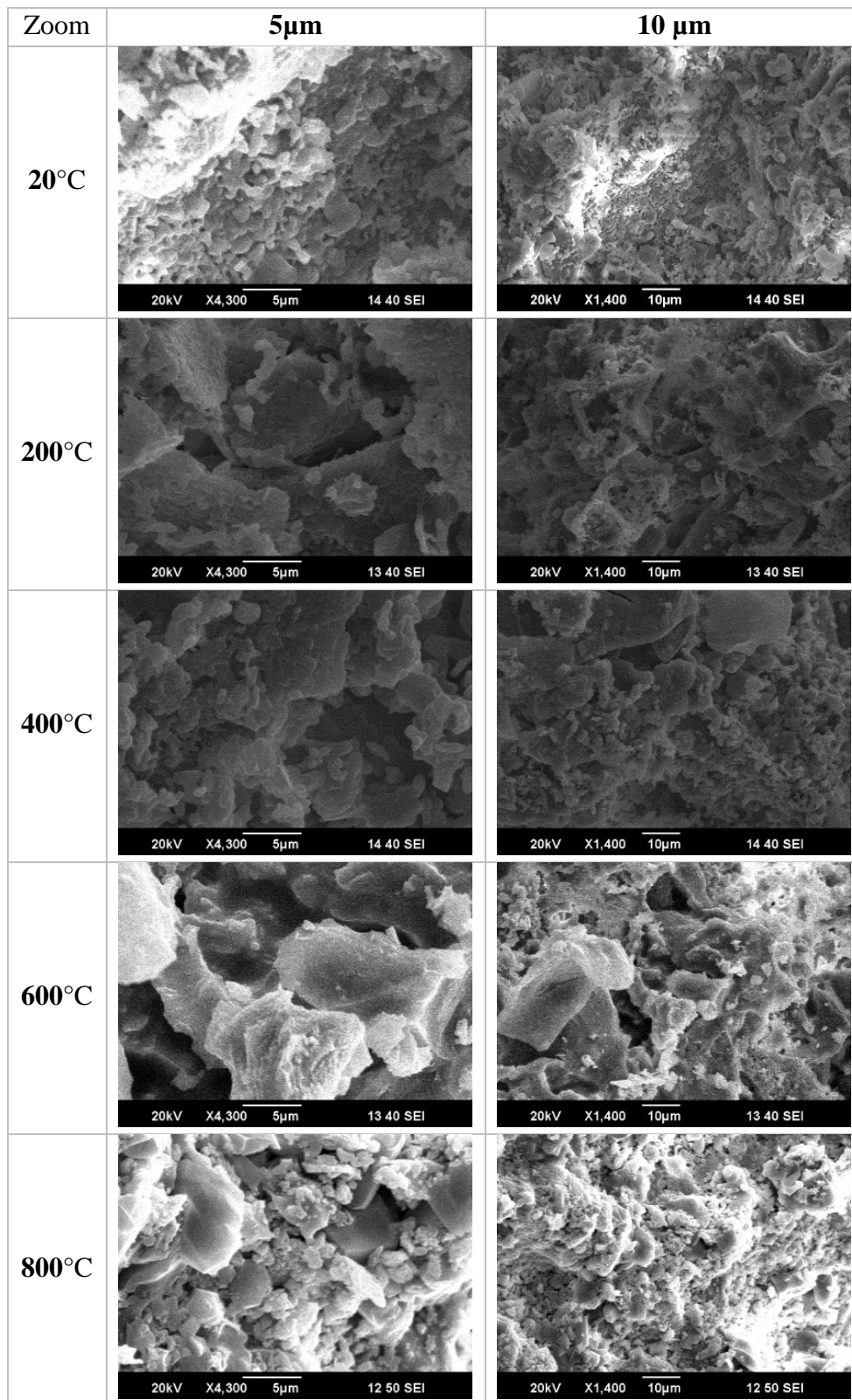


Fig 4.16: SEM micrographs of burnt masonry bricks (BB) at different temperatures

CONCLUSIONS AND RECOMMENDATIONS

5.1 General

This study was conducted to obtain the performance of burnt masonry bricks (BB) in terms of its mechanical properties at elevated temperatures and are compared with that of NSC and HSC. These material properties include compressive strength, splitting tensile strength, elastic modulus and stress-strain response. All the properties were measured at 24, 200, 400, 600 and 800°C temperatures at unstressed test conditions. Scanning electron microscope (SEM) analysis along with X-ray fluorescence (XRF) analysis was also carried out to study the microstructural changes and identification of elements in BB respectively. The data generated from these experimental studies is used to understand the performance of BB at elevated temperatures. The data is further used to formulate simplified mathematical relationships of mechanical properties of BB as a function of temperature. These relationships can be used as input parameters in computer programs for evaluating the fire resistance performance of structural members made up of BB.

5.2 Conclusions

Based on the results obtained from the above study, following conclusions are drawn:

- The compressive strength is gradually lost in burnt masonry bricks (BBs) with increase in temperatures, further there is slight variation in compressive strength results of BBs for both unstressed and residual test procedures.

- The loss in relative compressive strength is less for BBs compared to normal strength and high strength concrete (NSC and HSC) especially at temperatures higher than 400°C temperature.
- The high temperature splitting tensile strength of BBs is not much effected till 400°C temperature. Moreover, loss in relative tensile strength of BBs is lower compared to both NSC and HSC.
- The stress-strain response of BBs shows consistent post peak response at elevated temperatures depicting stable behavior of BBs before failure.
- The loss in elastic modulus of BBs is rapid initially but gradual at temperatures higher than 200°C, the modulus is also different from both NSC and HSC.
- The mineralogical transformations in BBs above 400°C are responsible for high porosity, fishers and cracking resulting in reduced strength at elevated temperatures.
- The high temperature material property relationships proposed for BBs can be used for analytical evaluations for structures made of BBs.

5.3 Recommendations

This research is novel in the field of “High Temperature Mechanical and Material Properties of Burnt Masonry Bricks” so further studies are required to fully analyze the complex behavior of mechanical properties of BB. The results emphasized that there is a need to do more in-depth research on the subject. The following are some of the key recommendations for future research works in this area:

- The mechanical properties of BB can be further refined by taking into account the significant factors such as change in permeability (pore structure), by Mercury Intrusion Porosimetry (MIP), which is the main factor of controlling the compressive strength.
- The performance of BB under stressed state conditions should also be checked.

- There should be comparative study mechanical properties of available different type of masonry bricks.

REFERENCES

- Abrams, M. S. (1971). "Compression strength of concrete at temperatures to 1600°F effect of temperature on concrete." *Portland Cement Association Research And Development*, 33-58.
- ACI Committee 216 (1997). "Standard Method for Determining Fire Resistance of Concrete and Masonry Construction Assemblies."
- ACI Committee 318 (2011). "Building code requirements for structural concrete and commentary."
- Andreini, M., and Sassu, M. (2011). "Mechanical behaviour of full unit masonry panels under fire action." *Fire Safety Journal*, 46(7), 440-450.
- Aramide, F. O. (2012). "Effect of firing temperature on mechanical properties of fired masonry bricks produced from ipetumodu clay." *Leonardo Journal of Sciences*, 11(21), 70-82.
- ASTM C67-14 (2014). "Standard Test Methods for Sampling and Testing Brick and Structural Clay Tile." ASTM International, West Conshohocken, PA.
- ASTM C1006-07 (2013). "Standard Test Method for Splitting Tensile Strength of Masonry Units." ASTM International, West Conshohocken, PA.
- ASTM C1314-14 (2014). "Standard Test Method for Compressive Strength of Masonry Prisms." ASTM International, West Conshohocken, PA.
- ASTM E111-04 (2010). "Standard Test Method for Young's Modulus, Tangent Modulus, and Chord Modulus." ASTM International, West Conshohocken, PA.
- ASTM E2309 (2011). "Standard Practices for Verification of Displacement Measuring Systems and Devices Used in Material Testing Machines." ASTM International, West Conshohocken, PA.

- Ayala, F. R. R. (2011). "Mechanical properties and structural behaviour of masonry at elevated temperatures." PhD Dissertation, University of Manchester, Oxford Road, Manchester M13 9PL, UK.
- Bažant, Z. P., Kaplan, M.F (1996). "Concrete at high temperatures: material properties and mathematical models." *London*, Longman (Addison-Wesley).
- Behnood, A., and Ghandehari, M. (2009). "Comparison of compressive and splitting tensile strength of high-strength concrete with and without polypropylene fibers heated to high temperatures." *Fire Safety Journal*, 44(8), 1015-1022.
- Brownell, W. E. (2012). *Structural clay products*, Springer Science & Business Media.
- Canadian Standard Association (2004). "S304. 1-04 Design of Masonry Structures." *Canadian Standards Association, Mississauga, Ontario, Canada*.
- Castillo, C., and Durrani, A. (1990). "Effect of transient high temperature on high-strength concrete." *ACI Materials journal*, 87(1), 47-53.
- Castillo, C., and Durrani, A. (1990). "Effect of transient high temperature on high-strength concrete." *ACI Materials Journal*, 87(1).
- Cheng, F.-P., Kodur, V., and Wang, T.-C. (2004). "Stress-strain curves for high strength concrete at elevated temperatures." *Journal of Materials in Civil Engineering*, 16(1), 84-90.
- Cultrone, G., Sebastián, E., Elert, K., De la Torre, M. J., Cazalla, O., and Rodríguez-Navarro, C. (2004). "Influence of mineralogy and firing temperature on the porosity of bricks." *Journal of the European Ceramic Society*, 24(3), 547-564.
- Drysdale, R. G., and Hamid, A. A. (2005). "Masonry structures: Behavior and design." *Mississauga, Ontario: Canadian Masonry Design Centre*.

- El-Mahllawy, M. S., and Kandeel, A. M. (2014). "Engineering and mineralogical characteristics of stabilized unfired montmorillonitic clay bricks." *HBRC Journal*, 10(1), 82-91.
- Elert, K., Cultrone, G., Navarro, C. R., and Pardo, E. S. (2003). "Durability of bricks used in the conservation of historic buildings - influence of composition and microstructure." *Journal of Cultural Heritage* 4(2), 91-99.
- Eurocode 6 (2005). "Eurocode 6 - Design of masonry structures - Part 1-2: General rules - Structural fire design." Avenue Marnix 17, B-1000 Brussels.
- Felicetti, R., Gambarova, P., Rosati, G., Corsi, F., and Giannuzzi, G. "Residual mechanical properties of high-strength concretes subjected to high-temperature cycles." *Proc., Proceedings, 4th International Symposium on Utilization of HS/H (Paris, France, 1996)*, 579-588.
- Fu, Y.-F., Wong, Y.-L., Poon, C.-S., Tang, C.-A., and Lin, P. (2004). "Experimental study of micro/macro crack development and stress–strain relations of cement-based composite materials at elevated temperatures." *Cement and Concrete Research*, 34(5), 789-797.
- Fu, Y., Wong, Y., Poon, C., and Tang, C. (2005). "Stress–strain behaviour of high-strength concrete at elevated temperatures." *Magazine of Concrete Research*, 57(9), 535-544.
- Gharrabi M., Velde B., and Sagon J.-P. (1998). "The Transformation of Illite to Muscovite in Pelitic Rocks: Constraints from X-ray Diffraction." *Clays and Clay Minerals*, 46, 79-88.
- Greenwood N.N., and Earnshaw A. (2006). *Chemistry of the Elements*, Oxford: Butterworth-Heinemann.
- Hachemi, S., and Ounis, A. (2014). "Performance of concrete containing crushed brick aggregate exposed to different fire temperatures." *European Journal of Environmental and Civil Engineering*(ahead-of-print), 1-20.

- Hatzinikolas, M., and Y. Korany (2005). "Masonry design for engineers and architects." *Edmonton, Alberta: Canadian Masonry Publications.*
- Husem, M. (2006). "The effects of high temperature on compressive and flexural strengths of ordinary and high-performance concrete." *Fire Safety Journal*, 41(2), 155-163.
- Johari, I., Said, S., Hisham, B., Bakar, A., and Ahmad, Z. A. (2010). "Effect of the change of firing temperature on microstructure and physical properties of clay bricks from Beruas (Malaysia)." *Science of Sintering*, 42, 245-254.
- Khaliq, W. (2012). "Performance characterization of high performance concretes under fire conditions." PhD Dissertation, Michigan State University, East Lansing, MI 48823, USA.
- Khaliq, W., and Kodur, V. (2012). "High temperature mechanical properties of high-strength fly ash concrete with and without fibers." *ACI Materials Journal*, 109(6).
- Khaliq, W., and Kodur, V. (2011). "High Temperature Properties of Fiber Reinforced High Strength." *ACI Special Publication*, 279.
- Khaliq Wasim, and Kodur Venkatesh (2011). "Thermal and mechanical properties of fiber reinforced high performance self-consolidating concrete at elevated temperatures." *Cement and Concrete Research*, 41(11), 1112-1122.
- Klosek-Wawrzyna, E., Malolepszy, J., and Murzyn, P. (2013). "Sintering Behavior of Kaolin with Calcite." *Procedia Engineering*, 57(1), 572-582.
- Kodur, V., Cheng, F.-P., Wang, T.-C., and Sultan, M. (2003). "Effect of strength and fiber reinforcement on fire resistance of high-strength concrete columns." *Journal of Structural Engineering*, 129(2), 253-259.
- Lee S., King K.J., Lee H.L., and Moon H.S. (2001). "Electron-Beam Induced Phase Transformations from Metakaolinite to Mullite Investigated By EF-TEM and HRTEM." *Journal of the American Ceramic Society*, 84, 2096-2099.

- Lie, T. T. (1992). "Structural Fire Protection." *ASCE Committee on Fire Protection*, Structural Division, New York, NY, 225-229.
- Mansoor, K. (2012). "2012 Pakistan garment factory fires." *The News*.
- Marrocchino, E., Rapti-Caputo, D., and Vaccaro, C. (2010). "Chemical–mineralogical characterisation as useful tool in the assessment of the decay of the Mesola Castle (Ferrara, Italy)." *Construction and Building Materials*, 24(12), 2672-2683.
- Mbumbia, L., and de Wilmars, A. M. (2002). "Behaviour of low-temperature fired laterite bricks under uniaxial compressive loading." *Construction and Building Materials*, 16(2), 101-112.
- Mbumbia, L., Mertens de Wilmars, A., and Tirlocq, J. (2000). "Performance characteristics of lateritic soil bricks fired at low temperatures: a case study of Cameroon." *Construction and Building Materials*, 14(3), 121-131.
- McConville C.J., and Lee W.E. (2005). "Microstructural Development on Firing Illite and Smectite Compared With that in Kaolinite." *Journal of the American Ceramic Society*, 88, 2267-2277.
- McConville C.J., Lee W.E., and Sharp J.H. (1998). "Comparison of Microstructural Evolution in Kaolinite Powders and Dense Clay Bodies." *British Ceramic Transactions*, 58, 75-92.
- Mezencevova, A., Yeboah, N. N., Burns, S. E., Kahn, L. F., and Kurtis, K. E. (2012). "Utilization of Savannah Harbor river sediment as the primary raw material in production of fired brick." *Journal of Environmental Management*, 113(1), 128-136.
- Millogo, Y., Hajjaji, M., and Ouedraogo, R. (2008). "Microstructure and physical properties of lime-clayey adobe bricks." *Construction and Building Materials*, 22(12), 2386-2392.
- Minitab (2013). "<http://www.minitab.com/en-us/>." *Release 17*.

- Nadjai, A., Garra, M. O., and Ali, F. (2003). "Finite element modelling of compartment masonry walls in fire." *Computers and Structures*, 81, 1923-1930.
- National Research Council of Canada (1965). "National building code of Canada." *Associate Committee on the National Building Code*, National Research Council, Ottawa.
- Nguyen, D., Meftah, F., Chammas, R., and Mebarki, A. (2009). "The behaviour of masonry walls subjected to fire: Modelling and parametrical studies in the case of hollow burnt-clay bricks." *Fire Safety Journal*, 44(4), 629-641.
- Noumowe, A. (2005). "Mechanical properties and microstructure of high strength concrete containing polypropylene fibres exposed to temperatures up to 200°C." *Cement and Concrete Research*, 35(11), 2192-2198.
- Paterson, M. S., and Wong, T.-f. (2005). *Experimental rock deformation-the brittle field*, Springer Science & Business Media.
- Phan, L. T. (1996). *Fire performance of high-strength concrete: A report of the state-of-the-art*, National Institute of Standards and Technology, Gaithersburg, Md, USA.
- Phan, L. T., Carino, N.J. (2000). "Fire performance of high strength concrete: research needs." *National Institute of Standards and Technology*.
- RILEM (1995). "129-MHT: Test methods for mechanical properties of concrete at high temperatures." *Materials and Structures*, 28, 410-414.
- RILEM TC 129-MHT: Test methods for mechanical properties of concrete at high temperatures Part 5: modulus of elasticity for service and accident conditions (2004). *MATERIALS AND STRUCTURES*, 37, 139-144.
- RILEM TC 129-MHT: Test methods for mechanical properties of concrete at high temperatures Part Part 4: tensile strength for service and accident conditions (2000). *MATERIALS AND STRUCTURES*, 33, 219-223.

- RILEM TC 200-HTC: Test methods for mechanical properties of concrete at high temperatures
Part 2: stress-strain relations (2007). *MATERIALS AND STRUCTURES*, 40, 855-864.
- Russo, S., and Sciarretta, F. (2013). "Masonry exposed to high temperatures: mechanical behaviour and properties—An overview." *Fire Safety Journal*, 55(1), 69-86.
- Russo, S., and Sciarretta, F. (2012). "Experimental and theoretical investigation on masonry after high temperature exposure." *Experimental Mechanics*, 52, 341-359.
- Sandoval, C., Roca, P., Bernat, E., and Gil, L. (2011). "Testing and numerical modelling of buckling failure of masonry walls." *Construction and Building Materials*, 25(12), 4394-4402.
- Schneider, U. (1988). "Concrete at High Temperatures-A General Review." *Fire Safety Journal*, 13(1), 55-68.
- Seynou, M., Millogo, Y., Ouedraogo, R., Traoré, K., and Tirloc, J. (2011). "Firing transformations and properties of tiles from a clay from Burkina Faso." *Applied Clay Science*, 51(1), 499-502.
- Shih, P. H., Wu, Z. Z., and Chiang, H. L. (2004). "Characteristics of bricks made from waste steel slag." *Waste Management*, 24, 1043–1047.
- Tang, W., and Lo, T. (2009). "Mechanical and fracture properties of normal-and high-strength concretes with fly ash after exposure to high temperatures." *Magazine of Concrete Research*, 61(5), 323-330.
- Wackerly, D. D., Mendenhall III, W., and Scheaffer, R. L. (2008). *Mathematical statistics with applications*, Thomson Higher Education, Belmont, CA, USA.
- Watstein, D. (1971). "Relation of unrestrained compressive strength of brick to strength of masonry." *Journal of Materials*, 6(2), 304.
- X'Pert High Score (1993). PANalytical B.V. Almelo, Netherlands.

Xiao, Z., Ling, T.-C., Poon, C.-S., Kou, S.-C., Wang, Q., and Huang, R. (2013). "Properties of partition wall blocks prepared with high percentages of recycled clay brick after exposure to elevated temperatures." *Construction and Building Materials*, 49(1), 56-61.

Yoshioka S., and Kitano Y. (1985). "Transformation of Aragonite to Calcite through Heating." *Geochemical Journal*, 19, 245-249.